



# **1 Gliding through marine heatwaves: Subsurface biogeochemical 2 characteristics on the Australian continental shelf**

3

4 Daneeja Mawren<sup>1,2,3\*</sup>, Julia Araujo<sup>4</sup>, Romain Le Gendre<sup>5</sup>, Jessica A. Benthuisen<sup>6</sup>, Franck Eitel  
5 Kemgang Ghomsi<sup>1,7,8</sup>, Jayanthi S. Saranya<sup>9</sup>, Amandine Schaeffer<sup>10,11</sup>

6

7 <sup>1</sup>Department of Oceanography, University of Cape Town, Cape Town, South Africa

8 <sup>2</sup>South African Environmental Observation Network, Egagasini Node, Roggebaai, South Africa

9 <sup>3</sup>Mascarene Environmental Consulting, Ltd, Mauritius

10 <sup>4</sup>National Center for Monitoring and Early Warning of Natural Disasters (CEMADEN), São José dos  
11 Campos, 12630-000, Brazil

12 <sup>5</sup>IFREMER, UMR 9220 ENTROPIE (IRD, Reunion Univ., IFREMER, New Caledonia Univ., CNRS), BP 32078,  
13 98897 Noumea Cedex, New Caledonia

14 <sup>6</sup>Australian Institute of Marine Science, Crawley, Western Australia 6009, Australia

15 <sup>7</sup>Geodesy Research Laboratory, National Institute of Cartography, P.O. Box 157, Yaoundé, Cameroon

16 <sup>8</sup>Centre for Earth Observation Science, University of Manitoba, Winnipeg, MB, Canada

17 <sup>9</sup>School of Earth and Environmental Sciences, College of Natural Sciences, Seoul National University, Seoul,  
18 Republic of Korea

19 <sup>10</sup>School of Mathematics and Statistics, University of New South Wales, Sydney, New South Wales, Australia

20 <sup>11</sup>Centre for Marine Science and Innovation, University of New South Wales, Sydney, New South Wales, Australia

21 \* Correspondence to: Daneeja Mawren ([daneejamawren@gmail.com](mailto:daneejamawren@gmail.com))

22

23

24



## 25 Abstract

26 Marine heatwaves (MHWs) disrupt ecosystems across multiple trophic levels by altering oxygen and biological  
27 productivity through the water column. Yet, most studies focus on the surface, overlooking subsurface processes that  
28 shape ecosystem responses, particularly under compound events involving multiple co-occurring extreme  
29 environmental conditions. To address this gap, we analysed 16 years of routine and event-based glider observations  
30 on the continental shelf around Australia to present the first comprehensive assessment of the subsurface  
31 biogeochemical response during surface MHWs across four contrasting coastal regions. Summer surface MHWs  
32 were characterised by a shallower mixed layer depth than normal conditions and enhanced stratification, confining  
33 warming to the upper ocean, while other seasons allow deeper penetration under weakly stratified conditions.  
34 Stratification favoured deeper and intensified deep chlorophyll maxima, aligned with the depth of stratification  
35 maxima, and emerged as a useful proxy for the vertical extent of MHWs. Across all regions and seasons, for  
36 non-MHW conditions, dissolved oxygen had a bimodal distribution above and below the mixed layer. However, this  
37 distribution changed with event severity and included greater concentrations of low dissolved oxygen and reduced  
38 concentrations of high dissolved oxygen during strong events. Below the mixed layer, the bimodal distribution was  
39 less apparent and oxygen concentrations during strong events were more concentrated towards middle values.  
40 During moderate and strong MHWs, chlorophyll concentrations declined in the mixed layer, albeit this trend was not  
41 apparent below it. Regional responses were related to the environmental setting, including the continental shelf  
42 structure and boundary current influences, underscoring the importance of region-specific monitoring to understand  
43 how MHWs influence biogeochemistry, and furthermore, their ecological consequences on coastal waters. The  
44 interaction between physical processes, such as seasonal circulation and stratification, and biological feedback,  
45 including the presence of deep chlorophyll maxima and potential oxygen production, highlights the complex  
46 biogeochemical responses to MHWs.

47

## 48 Keywords

49 Marine heatwaves; subsurface layers; stratification; biogeochemistry; chlorophyll; dissolved oxygen; glider  
50 observations; *in situ* measurements; coastal waters; continental shelf; Australia.

51

52

## 53 Short summary

54 Using sixteen years of ocean glider observations, we show that marine heatwaves shoal the mixed layer and alter  
55 subsurface biogeochemistry across Australia's continental shelf. While surface chlorophyll generally declined,  
56 strong stratification and event severity promoted deeper, intensified chlorophyll maxima while subsurface oxygen  
57 responses varied. These findings underscore the importance of region-specific dynamics in shaping ecological  
58 responses to marine heatwaves.



59

## 60 1. Introduction

61 As the Earth's climate continues to warm, the frequency and intensity of extreme events are increasing due to  
62 anthropogenic forcing (Frölicher et al., 2018; Laufkötter et al., 2020) with profound consequences for both  
63 ecosystems and human societies (Smith et al., 2021; 2023). Marine heatwaves (MHWs) are defined as long-lasting,  
64 extremely warm ocean temperature anomalies and have become an increasing focus of research for their important  
65 impacts on ecosystems. Recent studies have shown that subsurface signatures of MHWs can differ substantially  
66 from surface observations. For instance, during the 2019 North Pacific MHW (“The Blob”), subsurface warming  
67 persisted long after surface temperatures returned to normal, leading to prolonged ecological stress at depth (Amaya  
68 et al., 2020). Similarly, along the east coast of Australia in New South Wales (NSW), subsurface MHWs have been  
69 documented with minimal surface expression, highlighting the need for vertical profiling to fully capture subsurface  
70 dynamics (Schaeffer and Roughan, 2017; Schaeffer et al., 2023). Investigating the subsurface dynamics of MHWs in  
71 coastal areas is critical for assessing ecological and socio-economic impacts.

72

73 In coastal regions and over continental shelves, subsurface biogeochemical processes play a central role in  
74 sustaining vital ecosystem services such as biodiversity, carbon sequestration and nutrient cycling, while supporting  
75 economic activities such as fisheries and aquaculture (Walsh, 1991; Siefert and Plattner, 2004; Marre et al., 2015).  
76 When combined with MHWs, biogeochemical extremes can trigger severe ecological disruption, amplifying  
77 existing environmental stressors, such as nutrient limitation (Cavole et al., 2016; Le Grix et al., 2020), acidification,  
78 and deoxygenation (Tassone et al., 2022), ultimately reducing productivity and threatening marine ecosystem health.

79

80 Understanding how MHWs influence key biogeochemical variables, such as chlorophyll-a concentrations and  
81 oxygen levels, is essential for predicting ecosystem responses. For instance, nutrient scarcity during MHWs can  
82 limit phytoplankton growth, while warmer waters increase metabolic demands in marine species, further straining  
83 ecosystems (Chen et al., 2023). Although surface chlorophyll-a often decreases during MHWs (Le Grix et al., 2020),  
84 responses vary depending on factors such as latitude and nutrient availability (Sen Gupta et al., 2020; Noh et al.,  
85 2022). In regions where stratification limits nutrient upwelling, phytoplankton productivity may decrease, whereas,  
86 at higher latitudes, stratification can enhance productivity by maintaining phytoplankton in the sunlit surface layers  
87 (Kwiatkowski et al., 2020). On a global scale, MHWs have been found to promote the development of deep  
88 chlorophyll maxima, based on 17 years of biogeochemical-Argo float data (Ma and Chen, 2025). Reduced dissolved  
89 oxygen during MHWs represents another critical issue, particularly in shallow coastal areas. Warmer water  
90 temperatures decrease oxygen solubility, potentially leading to hypoxic conditions that can severely affect marine  
91 life (Meier et al., 2018; Safonova et al., 2024). MHWs intensify this mismatch between oxygen supply and demand,  
92 as respiration rates increase in response to higher temperatures, further depleting oxygen levels (Tassone et al.,  
93 2022). Combined effect of MHWs, reduced oxygen levels, and habitat compression can trigger mass mortality



94 events across multiple taxa, including fish, seagrasses, and marine mammals (Sampaio et al., 2021; Holbrook et al.,  
95 2022), while altered prey distribution and increased metabolic demands can produce cascading effects throughout  
96 marine food webs (Smith et al., 2023; Gomes et al., 2024).

97

98 While long-term satellite-derived records of sea surface temperature (SST) and surface chlorophyll-a have advanced  
99 our understanding of MHWs globally, they require concurrent in water measurements to assess the extent of  
100 subsurface temperature extremes and biogeochemical changes given the range of ecological impacts that can occur  
101 through the water column (Smith et al., 2023). Traditional *in situ* methods such as moored temperature  
102 measurements, conductivity-temperature-depth, and expendable bathythermograph casts can provide vertical  
103 profiles, but these observations are often limited in spatial and temporal coverage (Oliver et al., 2021; Malan et al.,  
104 2025; Le Gendre et al., 2025) and rarely include biogeochemical observations. In addition, coastal numerical models  
105 offer valuable simulations of subsurface thermal structures, but they require large amounts of high-resolution data  
106 for validation or assimilation, as they remain prone to uncertainties in poorly observed regions (Lachkar et al.,  
107 2019).

108

109 Ocean gliders offer a major advancement in subsurface monitoring, through high-resolution, autonomous, and  
110 continuous measurements of water temperature, salinity, and biogeochemical properties, including dissolved oxygen  
111 and chlorophyll fluorescence (Testor et al., 2019). Although glider deployments have limited temporal coverage for  
112 detecting extremes, their ability to sample across depths and regions provides an unprecedented view in shelf and  
113 boundary current environments (Testor et al., 2019), thus providing the means to measure simultaneously  
114 oceanographic variables, stratification, phytoplankton, and oxygen dynamics at depth. Furthermore, event-based  
115 approaches, where gliders are deployed specifically to sample MHWs, can provide real-time, dynamic insights into  
116 the subsurface evolution and intensity of these events, delivering essential input to immediate ecosystem response  
117 strategies (Davies et al., 2021; Benthuyssen et al., 2025). Previous studies have made notable strides on better  
118 understanding the subsurface dynamics and biogeochemical variability using gliders off the Australian coast  
119 (Pattiaratchi et al., 2011; Schaeffer et al., 2016a,b; Chen et al., 2019; Chen et al., 2020; Ridgway and Ling, 2023).  
120 However, these works focus on specific regions off the Australian coast or were limited to “short-term”  
121 observations.

122

123 To address this gap, our study leverages data from the Australian Integrated Marine Observing System (IMOS)  
124 gliders which provide high-resolution subsurface observations along the Australian continental shelf since 2007  
125 (Pattiaratchi et al., 2017). By combining these repeated glider measurements with satellite-derived surface data, we  
126 aim to provide a seasonal and regional comparison across four distinct Australian shelf regions, highlighting broader  
127 patterns of subsurface MHW characteristics and their impacts on key biogeochemical variables. Specifically, we test  
128 the following hypotheses: (1) surface MHWs can lead to reduced chlorophyll concentrations and lower dissolved  
129 oxygen levels at the surface; (2) despite surface reductions, MHWs may promote deeper chlorophyll maxima and



130 higher dissolved oxygen concentrations at depth, potentially via enhanced subsurface productivity; (3) the depth  
131 extent of surface MHWs varies with regions and seasons, and therefore establishing seasonal and regional baselines  
132 are important to interpret anomalies; and (4) the severity of MHW-induced stratification modulates biogeochemical  
133 variables (dissolved oxygen and chlorophyll).

134

135 The following sections outline our approach and findings: Sect. 2 describes the SST and glider datasets, statistical  
136 methods, and MHWs metrics. Section 3.1 describes the characteristics of surface MHWs in the study regions.  
137 Hypotheses (1) and (2) are examined in Sect. 3.2, which investigates how MHW severity influences chlorophyll and  
138 dissolved oxygen within and below the surface mixed layer. Hypothesis (3) is addressed in Sect. 3.3, where we  
139 explore regional and seasonal variations in the depth extent of MHWs, stratification and associated biogeochemical  
140 profiles. Hypothesis (4) is evaluated across Sects. 3.2 and 3.3, which together assess how MHWs modulates  
141 subsurface biogeochemical signatures in different regimes, based on their stratification, chlorophyll and oxygen  
142 regimes. Finally, Sect. 4 discusses these findings in the context of previous global and Australian studies, leading to  
143 the Conclusions in Sect. 5.

144

145

## 146 2. Data and Methods

### 147 2.1 Satellite dataset and surface MHW detection

148 Given the coastal scale of our study, we used the National Oceanic and Atmospheric Administration (NOAA)  
149 CoralTemp v3.1<sup>1</sup> Sea Surface Temperature (SST) product, which integrates three L4 satellite SST analysis products,  
150 to provide a global, daily, gap-free gridded, night-time SST field at 0.05° horizontal resolution since 1985 (Skirving  
151 et al., 2020). This dataset is used to track surface MHWs in near real-time<sup>2</sup> using the definition and criteria of  
152 Hobday et al., (2016), which detects temperature events exceeding a locally determined upper threshold of the 90th  
153 percentile relative to the long-term day-of-the-year climatology for a minimum of five consecutive days, with no gap  
154 of more than two days. The baseline climatological period was defined here as a 30-year period between 1985 and  
155 2014, following recommendations of Hobday et al. (2016). The MHW detection and analysis were performed using  
156 the Python module available at <https://github.com/ecjoliver/marineHeatWaves>. We extracted the SST dataset over  
157 the period from 1 January 1985 to 30 June 2025 and the following MHW metrics were analysed over our study  
158 period from 2009 to mid-2025: the total number of events, the mean duration of the MHW events, and the mean  
159 severity of the MHW (Eq. 1; following Sen Gupta et al., 2020).

160

<sup>1</sup> CoralTemp v3.1 product's website: <https://coralreefwatch.noaa.gov/product/5km/index.php>.

<sup>2</sup> NOAA Coral Reef Watch marine heatwave website: [https://coralreefwatch.noaa.gov/product/marine\\_heatwave/](https://coralreefwatch.noaa.gov/product/marine_heatwave/).



## 161 2.2 Glider dataset

162 To assess the subsurface structure of MHWs, our study benefited from the Australian national glider data acquisition  
163 strategy set up in 2007 by the Ocean Gliders facility under the Australia's Integrated Marine Observing System  
164 (IMOS; Pattiaratchi et al., 2017). Subsequently, IMOS enabled the routine deployment of gliders on the continental  
165 shelves around Australia for sustainable observations. This facility has been augmented by event-based sampling of  
166 MHWs since December 2018 (Benthuisen et al., 2025), delivering subsurface measurements of oceanographic  
167 parameters along with other near-real time platforms during events (e.g. Box 2 of Capotondi et al., 2024). Ocean  
168 gliders are autonomous vehicles which alter their buoyancy to travel up and down the water column while sampling  
169 seawater properties (Rudnick, 2016). We used data from IMOS using Teledyne Webb Research Slocum Electric  
170 Gliders (G1, G2 and G3), equipped with Seabird-CTD, WETLabs BBFL2SLO 3 Eco Puck sensor measuring  
171 chlorophyll fluorescence, colored dissolved organic matter (CDOM) and 660 nm backscatter, and an Aanderaa  
172 Oxygen optode (Pattiaratchi et al., 2011; Chen et al., 2020). Missions typically last between three to five weeks,  
173 with a maximum depth of 200 m. For this study, we focus on measurements of ocean temperature, salinity,  
174 chlorophyll-a fluorescence (proxy for phytoplankton concentration; Blondeau-Patissier et al., 2014), and dissolved  
175 oxygen. The measurements undertake a delayed-mode quality control (Woo and Gourcuff, 2023) and are made  
176 publicly available through IMOS on the Australian Ocean Data Network (AODN) Portal<sup>3</sup>.

177

## 178 2.3 Study regions

179 The analysis of all available deployments led us to the definition of four main regions of interest encompassing the  
180 highest density of gliders transects between 2009 and 2025: (i) northeastern Australia off Queensland (QLD),  
181 confined within the limits of 144.7° E to 148.0° E and 13.3° S to 19.7° S; (ii) southeastern Australia off New South  
182 Wales (NSW), from 149.7° E to 154.7° E and 28.5° S to 36.7° S; (iii) southwest Western Australia (SW WA), from  
183 113.2° E to 116.1° E and 29.1° S to 33.5° S; and (iv) the eastern coast of Tasmania (TAS), from 146.8° E to 149.5° E  
184 and 40.5° S to 44.6° S (Fig. 1). These regions encompass contrasting continental shelf systems influenced by distinct  
185 physical processes, enabling us to assess how MHWs impact biogeochemical conditions under different dynamics.

---

<sup>3</sup> Australian Ocean Data Network (AODN) website: <https://portal.aodn.org.au/>.

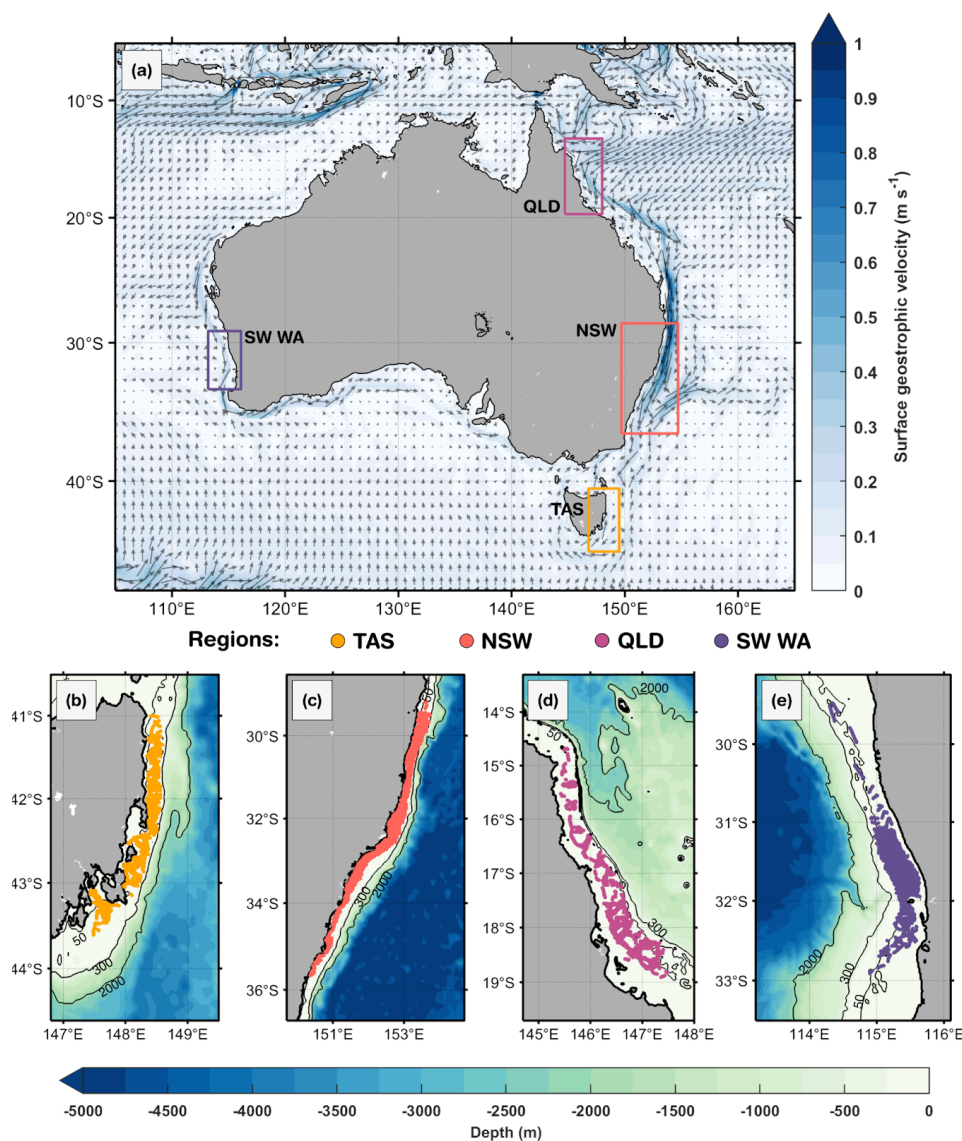


**Figure 1.** Study regions off the Australian coast. (a) Mean surface geostrophic currents (arrows) and highlighted boxes for each region of interest: northeastern Australia (Queensland region, QLD), southeastern Australia (New South Wales, NSW), southwest Western Australia (SW WA) and eastern Tasmania (TAS). Gliders' profile positions are illustrated in each zoomed region: (b) TAS, (c) NSW, (d) QLD and (e) SW WA. In (a), the annual mean geostrophic currents were based on 1993 to 2020 and provided by the Integrated Marine Observing System (IMOS, <https://imos.aodn.org.au/oceancurrent>). Isobaths of 50 m, 300 m, and 2000 m are shown in (b-e), derived from ETOPO1 bathymetry (Eakins & Sharman, 2010).





## 187 2.4 Profile selection and data processing

188 Glider deployments were selected to keep only those profiles within the aforementioned study regions, spanning a  
 189 16-year period from January 2009 to June 2025. To ensure the quality of our analyses, the following quality control  
 190 steps were taken: (i) selection of only ‘good data’ flags<sup>4</sup>; (ii) removal of chlorophyll outliers; (iii) applying a step to  
 191 address non-photochemical quenching in chlorophyll observations; and (iv) removal of data points inside the  
 192 bottom boundary layer (BBL). To remove the noise from the chlorophyll measurements (step (ii)), the outliers were  
 193 identified based on a moving average of window size equivalent to 1,000 points, discarding values above two  
 194 standard deviations of the logarithmic chlorophyll. Moreover, light-induced fluorescence leads to errors in sensor  
 195 measurements of phytoplankton concentration (quenching), causing high variability in chlorophyll-a fluorescence  
 196 profiles. To mediate this effect (step (iii)), we used only night-time data points, defined as any time before sunrise or  
 197 after sunset (as in Schaeffer et al., 2016b). Regarding the variable BBL contamination due to sloping topography, we  
 198 removed data within 20 m above the seabed, similar to Schaeffer et al. (2014, 2017). This threshold aims to  
 199 minimize contamination from interference in the near-bottom levels when aggregating the shelf profiles over various  
 200 topographic depths for a combined analysis.

201

202 This study is focused on continental shelves, and hence the rare measurements from deeper regions were excluded.  
 203 Off QLD and SW WA, only measurements over bathymetry between 40 and 80 m were retained. For regions with  
 204 deeper and steeper continental shelves, i.e. TAS and NSW, we retained measurements between 50 and 120 m.  
 205 Finally, we separated the data points into downward and upward casts, binned each cast into a 1 m vertical  
 206 resolution, averaged each pair of down/upward casts, and binned the averaged profiles into fixed distances of 1 km  
 207 horizontal resolution, which is more than the median distance between profiles (e.g. 100–200 m in NSW region,  
 208 Schaeffer et al., 2016b). These last steps enable vertical and horizontal consistency of profiles, avoid glider’s  
 209 direction bias when averaging the down/upward casts, and reduce noise for shelf-scale comparison of subsurface  
 210 MHW signals. In Fig. S1, we illustrate a glider mission before and after quality control steps mentioned above.

211

212

## 213 2.5 Classifying MHW vs non-MHW profiles

214 We classify MHW and non-MHW glider profiles by first collocating MHW severity index in time and space using  
 215 the satellite SST dataset. Thus, the severity index (S) was calculated for each profile following Sen Gupta et al.  
 216 (2020), as below:

$$217 \quad S_{i,d} = \frac{SST_{i,d} - SST_{i,d}^{clim}}{SST_{i,d}^{PC90} - SST_{i,d}^{clim}} \quad (1)$$

4

218 [https://content.aodn.org.au/Documents/IMOS/Facilities/Ocean\\_glider/Delayed\\_Mode\\_QAQC\\_Best\\_Practice\\_Manual\\_OceanGliders\\_LATEST.pdf](https://content.aodn.org.au/Documents/IMOS/Facilities/Ocean_glider/Delayed_Mode_QAQC_Best_Practice_Manual_OceanGliders_LATEST.pdf)





where  $SST_{i,d}^{clim}$  is the long-term daily mean SST on the  $d$ th day of the year at location  $i$ ,  $SST_{i,d}^{PC90}$  is the 90<sup>th</sup> percentile of SST on the same day and location as the glider profile. The MHWs were categorized into four types: (i) moderate,  $1 < S \leq 2$ ; (ii) strong,  $2 < S \leq 3$ ; (iii) severe,  $3 < S \leq 4$ , and (iv) extreme ( $S > 4$ ) following the category indices proposed in Hobday et al. (2018). For each study region, the mean location of the glider profiles was determined, and time series of the severity index were derived, enabling the representation of an ‘average’ severity timeline for each region (see Figs. 1b-e).

Then, using glider data, the seasonal climatology at each depth was computed for each region by averaging profiles over 3-month periods (austral summer - December/January/February, autumn - March/April/May, winter - June/July/August, and spring - September/October/November). Note that the profiles showing negative seasonal anomalies *in situ* surface temperature were excluded from the satellite-based MHW classification. These discrepancies may arise due to different datasets used, methodology when computing anomalies and also due to the sampling locations of these profiles. For instance, given the wide area selected for New South Wales, the southern part of the region is cooler than the northern region. As a result, in comparison to the mean profile, the southern profiles may potentially present a cool anomaly.

235

## 2.6 *In situ* subsurface parameters

To further characterize the surface-MHWs in subsurface layers, some proxies were defined, such as: (i) MHW depth extent, as the depth of positive temperature anomalies based on the seasonal regional mean temperature profile; (ii) mixed layer depth (MLD); (iii) thermocline depth; (iv) depth of maximum stratification, defined as the depth at which the buoyancy frequency reaches its maximum value in the water column; (v) depth of deep chlorophyll maxima (DCM); and (vi) dissolved oxygen saturation.

242

The MLD was computed for each individual temperature profile by identifying the shallowest depth at which the absolute temperature difference from the surface (0 m) exceeded a fixed threshold of 0.2° C. This threshold-based method is commonly applied to *in situ* observations due to its physical relevance in stratified ocean conditions (e.g., de Boyer Montégut et al., 2004). Profiles with missing surface data or insufficient vertical resolution near the surface were excluded from MLD calculations. MLD estimates were then averaged seasonally and grouped into MHW and non-MHW categories, based on the presence or absence of MHW conditions.

249

The thermocline depth was computed from the vertical temperature profiles by calculating the temperature gradient with respect to depth. The depth corresponding to the maximum negative gradient (i.e. the strongest rate of temperature decrease with depth) was defined as the thermocline depth.

253



254 The buoyancy frequency, also called the Brunt Väisälä frequency, represents the degree of stratification and is  
 255 defined as:

$$256 \quad N^2 = -\frac{g}{\rho_0} \frac{\partial \rho}{\partial z} \quad (2)$$

257 where  $\rho_0$  represents the background density,  $g$  is the gravitational constant and  $\frac{\partial \rho}{\partial z}$  denotes the vertical gradient of  
 258 potential density. The density was calculated from the glider's vertical temperature and salinity profiles.

259

260 Dissolved oxygen saturation was computed from temperature, salinity and pressure following standard solubility  
 261 formulations, using the García and Gordon (1992) equation for seawater. Hence, oxygen saturation was calculated as  
 262 the ratio between measured dissolved oxygen concentration and the corresponding solubility value at in-situ  
 263 conditions. This provides a temperature- and salinity-adjusted measure of oxygen availability relative to atmospheric  
 264 equilibrium, making it a useful indicator of both biogeochemical processes (production and respiration) and physical  
 265 transport mechanisms (vertical mixing and horizontal advection) that influence oxygen independently of solubility  
 266 changes.

267

268 To evaluate the relationships between physical and biogeochemical variables during MHWs, we calculated the  
 269 correlations by regions and seasons separately. The variables considered include MHW depth extent, depth of  
 270 maximum stratification, deep chlorophyll maximum (DCM) depth, thermocline depth, dissolved oxygen (DOX)  
 271 anomalies, chlorophyll (CPHL) anomalies, and temperature anomalies above and below the MLD. Several  
 272 restrictions were applied to ensure that the correlations were unbiased.

273 (a) All MHW profiles were included to increase the number of data points and improve statistical  
 274 robustness.

275 (b) Depths shallower than 5 m and within 5 m of the bottom (based on the maximum depth after QC), were  
 276 excluded for all depth-related metrics (thermocline depth, MHW depth extent, DCM depth, and depth  
 277 of stratification maximum) to avoid surface and near-bottom artefacts.

278 (c) Only stratified profiles were retained following the following methodology:

- 279 (i) Identify the depth of maximum stratification,
- 280 (ii) Calculate the seasonal 25<sup>th</sup> percentile of stratification,
- 281 (iii) Profiles exceeding this threshold were classified as stratified.

282 This approach excludes winter or homogeneous profiles that would otherwise give false strong correlations.

283 (d) Correlations were considered significant only if the p-value was less than 0.005 and the number of data  
 284 points was greater than 30.

285 (e) The MHW depth was calculated as follows:

- 286 (i) Identify the last positive temperature anomaly from the surface before it turns negative,
- 287 (j) Discard profiles where the entire temperature anomaly profile was entirely negative or  
 288 positive (i.e. discard well-mixed profiles).



289

## 290 2.7 Summary of glider missions in surface MHWs

291 Across the four study regions, a total of 202 glider missions were recorded over the continental shelf between  
 292 January 2009 and June 2025, with the highest number off SW WA (77 glider missions) and NSW (56 missions),  
 293 followed by TAS (41 missions) and QLD (27 missions). These missions yielded 61,280 profiles (Table 1), with  
 294 NSW and SW WA contributing the largest to the dataset (19,785 and 19,355 profiles, respectively), and fewer  
 295 profiles in TAS (11,699) and QLD (10,441). These glider missions and their associated profiles were distributed  
 296 seasonally, with and without MHW encounters (Table 1, Figs. 2b, d, f, h). Note that the number of chlorophyll  
 297 profiles is lower than for other variables because of (i) quality control steps, (ii) removal of chlorophyll outliers and  
 298 (iii) fluorescence quenching as described in sect. 2.4, and these data are presented in Supplementary Table S1.

299

300 **Table 1. Seasonal number of profiles with and without MHWs by region, as northeastern Australia (Queensland region,**  
 301 **QLD), southwest Western Australia (SW WA), southeastern Australia (New South Wales, NSW) and eastern Tasmania**  
 302 **(TAS).**

		Number of profiles				
		Summer (DJF)	Autumn (MAM)	Winter (JJA)	Spring (SON)	Total profiles
<b>QLD</b>	MHW	788	2,269	894	619	<b>10,441</b>
	Non MHW	1,697	953	1,300	1,921	
	<b>Total</b>	<b>2,485</b>	<b>3,222</b>	<b>2,194</b>	<b>2,540</b>	
<b>SW WA</b>	MHW	953	512	187	139	<b>19,355</b>
	Non MHW	3,751	4,251	5,611	3,951	
	<b>Total</b>	<b>4,704</b>	<b>4,763</b>	<b>5,798</b>	<b>4,090</b>	
<b>NSW</b>	MHW	294	989	342	1,167	<b>19,785</b>
	Non MHW	2,019	3,283	4,675	7,016	
	<b>Total</b>	<b>2,313</b>	<b>4,272</b>	<b>5,017</b>	<b>8,183</b>	
<b>TAS</b>	MHW	499	1,007	31	150	<b>11,699</b>
	Non MHW	1,450	2,535	2,181	3,846	
	<b>Total</b>	<b>1,949</b>	<b>3,542</b>	<b>2,212</b>	<b>3,996</b>	

303

304 NSW recorded the greatest number of MHW missions, with 12 separate glider deployments encountering MHW  
 305 conditions in spring and 10 in autumn (Fig. 2d), corresponding to 1,167 and 989 MHW profiles, respectively (Table



1). In SW WA, most missions and profiles occurred in winter and autumn, yet MHW missions (profiles) were more frequent in summer (10 MHW gliders; 953 MHW profiles) and autumn (7 MHW gliders; 512 MHW profiles) (Fig. 2h, Table 1). TAS also recorded the highest number of MHW profiles in autumn (1,007 profiles, over 7 missions) and summer (499 profiles, over 5 missions) (Fig. 2b, Table 1). In contrast, QLD showed missions with a more even seasonal spread (Fig. 2f; Table 1), with MHW gliders and profiles more common in winter (5 missions; 894 profiles) and autumn (5 missions; 2,269 profiles), this last season being the greatest number of MHW profiles among all seasons and regions. Despite an overall lower number of MHW missions in QLD, the proportion of MHW profiles relative to the total profiles was higher compared to other regions (Figs. 2e, g, Table 1). This reflects the fact that MHWs in QLD are longer-lasting (Fig. 3h), and therefore glider deployments are more likely to capture them.

The vertical distribution of glider profiles also varied across regions due to distinct sloping topography (Figs. 2a, c, e, g), with the highest profile density extending to depths of up to 100 m off TAS and NSW, while profiles were generally shallower (mostly less than 60 m) off QLD and SW WA. MHW profiles, although consistently fewer than non-MHW profiles, were more frequent in the upper 20 m (Figs. 2a, c, e, g) than at the surface or at deeper layers. To ensure a robust representation of the vertical structure, profiles were truncated at depths where less than 10% of profiles were available (and 20% for QLD and SW WA), resulting in a maximum analysed depth of 90 m for NSW and TAS, 40 m for QLD, and 30 m for SW WA.

The severity of MHW profiles further highlighted regional differences (Fig. 2i). Most events were classified as Category 1 (“Moderate”), with the highest numbers recorded in QLD (3660 profiles) and NSW (2472 profiles). Category 2 (“Strong”) MHWs were most frequently sampled off QLD with 910 profiles, followed by 320 profiles off NSW, 203 profiles off TAS, and 134 profiles off SW WA. Category 3 (“Severe”) events were rare and only sampled off TAS (11 profiles), while Category 4 (“Extreme”) events were not sampled over the continental shelf after quality control steps. Together, these patterns reflect regional contrasts in the number of glider missions, the seasonal and vertical distribution of profiles, and the severity of MHW conditions observed.

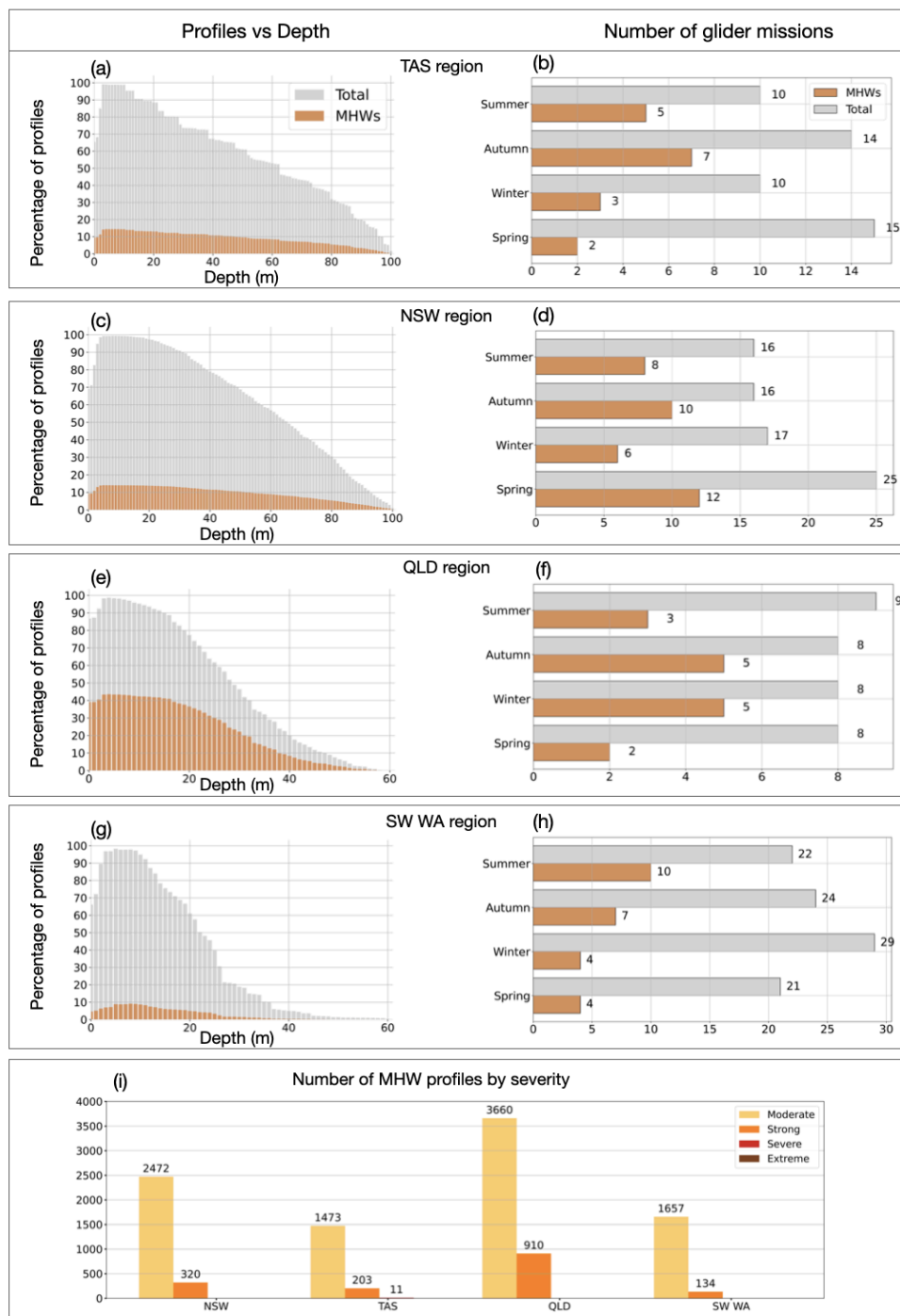




Figure 2. (a,c,e,g) Depth distribution of profiles for Tasmania (TAS), New South Wales (NSW), Queensland (QLD) and southwest Western Australia (SW WA), showing the percentage of total profiles (grey) and MHW profiles (orange) at each depth. (b,d,f,h) Seasonal counts of glider missions for each region, with total missions in grey and MHW missions in orange. (i) Number of MHW profiles per region, classified by severity: moderate, strong, severe and extreme. A glider is classified as being in a MHW based on its position and whether a surface MHW was identified there from the NOAA CoralTemp v3.1 SST with a reference period of 1985-2014.

### 3. Results

#### 3.1 Characteristics of surface marine heatwaves

Regional variations in surface MHW metrics derived from satellite SST are illustrated in Fig. 3. From 2009 to mid-2025, the eastern Tasmanian coast (TAS) experienced over 80 surface MHWs (Fig. 3a), whereas fewer than 40 events were detected along the continental shelf. Around Storm Bay in southeast TAS (43° S, 147.5° E), where most gliders were initially deployed, MHWs were generally long-lasting with mean durations of 27-31 days and mean severity exceeding 1.80 (Figs. 3b, c). To better capture the temporal distribution of MHWs relative to glider sampling, a timeline analysis was performed for each region (Fig. 4). MHWs in the TAS region were most frequent from November through to April, with strong to severe events concentrated between January and February (Fig. 4a). In several instances, glider profiles sampled prolonged, strong to severe (Fig. 2i) MHWs, with severity indices exceeding 3, including April 2016, February 2019, January 2022, and December 2023.

Relative to other Australian regions, NSW exhibited the highest occurrence of MHWs, with more than 100 MHWs detected over the study period (Fig. 3d). This highly dynamic region is typically characterised by short-lived MHWs lasting less than 10 days (Fig. 3e). On the inner shelf, the mean severity of MHWs in NSW did not exceed 1.65, which is lower than that observed off TAS. However, two short-lived but severe events in September 2013, and October 2018 (Fig. 4c), exceeded a severity index of 3. Glider missions deployed during these periods sampled through the tail of the events, capturing a maximum severity value of 2.1 and 1.6, respectively.

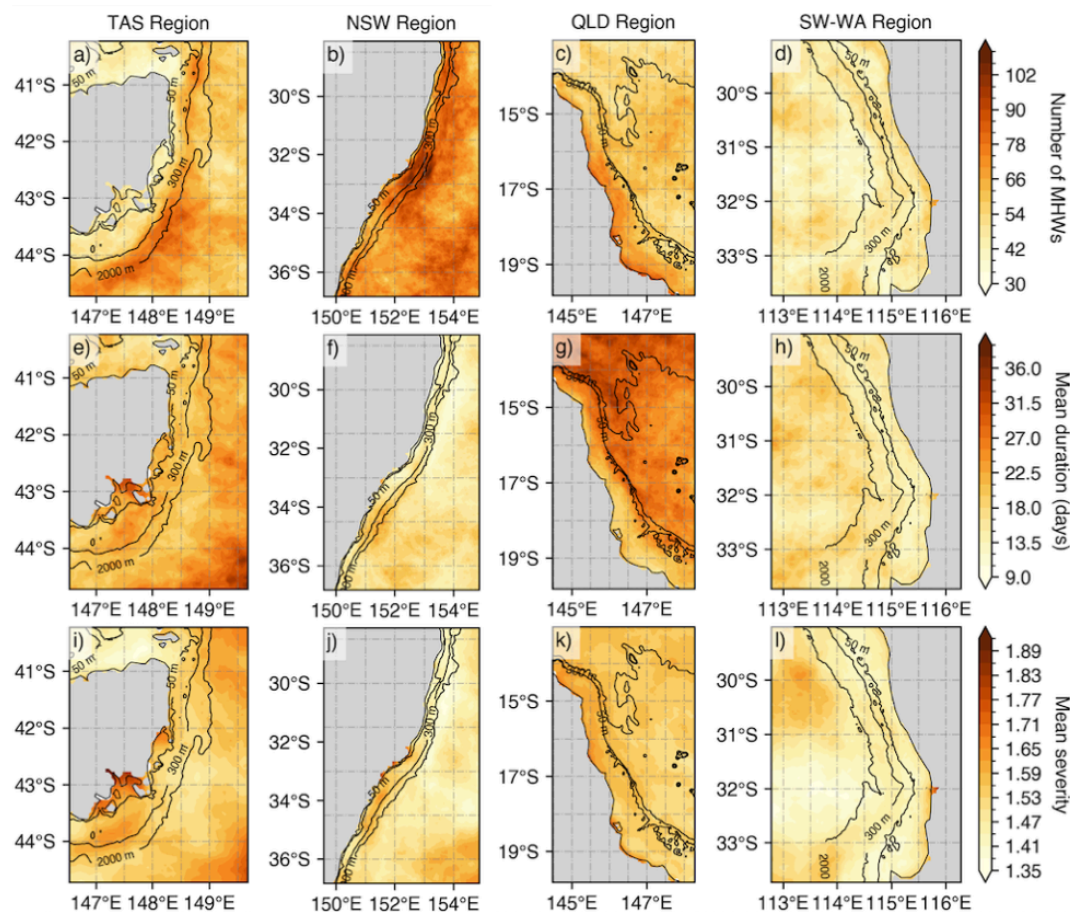


Figure 3. Mean surface MHW metrics based on NOAA CoralTemp v3.1 (climatology 1985–2014 reference period) over the gliders' deployment period (1 January 2009 – 30 June 2025) by regions: (a–e–i) eastern Tasmania (TAS), (b–f–j) southeastern Australia (New South Wales, NSW), (c–g–k) Queensland region (QLD), and (d–h–l) southwest Western Australia (SW WA). The top panels represent the number of MHWs, the middle panels show the mean duration (in days), and bottom panels indicate the mean MHW severity.

Off northeast Australia (north of 20°S), MHWs were more frequent over the continental shelf, with 66–78 occurrences recorded, compared to fewer events in offshore waters (Fig. 3g). In agreement with the higher frequency, MHWs on the shelf were shorter in duration (Fig. 3h), while offshore events were generally more prolonged, lasting 28–36 days on average. Across the central to northern GBR off QLD, the severity of MHWs typically had mean values below 1.65. However, there have been events with longer duration and higher severity over the continental shelf, particularly between autumn and winter, in the past decade (Fig. 4d). These intense





seasonal events also coincided with a higher proportion of MHW gliders during these seasons (Fig. 2g). The 2016 MHW stood out as a prolonged (more than 5 months) and severe event captured by three glider missions that sampled the onset (maximum severity: 2.6), middle (maximum severity: 2.3) and tail (maximum severity: 2.6) of the event. Additional severe MHWs were also sampled in March 2017 (maximum severity: 2.9) and September 2022 (maximum severity: 2.1). It is important to note that while some deployments shown in Fig. 4 coincided with severe satellite-detected MHWs, several profiles were excluded during quality control, and therefore may not fully reflect peak severity of the event.

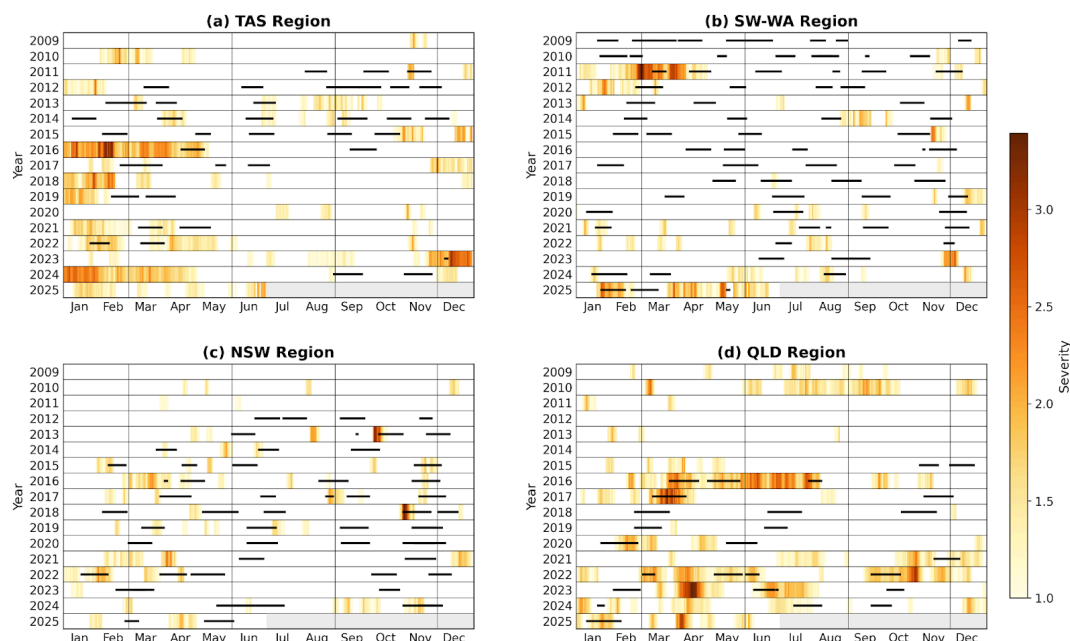
382

In contrast to eastern Australia, MHWs off the SW WA were shorter (less than 10 days on average; Fig. 3k), less frequent with less than 45 MHWs recorded (Fig. 3j) and generally weaker in severity ranging between 1.3-1.5 (Fig. 3l). The low severity of MHWs in SW WA appears to be influenced by periods of sustained MHW cold spells off the west coast, which contributed to the lower mean values over the study period (Feng et al., 2021). Such prolonged and cold events can dampen the long-term mean MHW metrics, while other regions in eastern Australia experience a higher prevalence of MHWs with greater duration and intensity. As indicated by the number of glider missions and MHW profiles (Fig. 2h and Table 1), events in SW WA were more frequent and severe between summer and autumn (Fig. 4b). These seasonal peaks coincided with increased glider sampling efforts that complemented satellite observations. The prolonged 2011 MHW is a key event in the region marked by strong to extreme severity nearshore. This event was sampled by two glider missions, one in March (maximum severity: 2.1) and the other in April (maximum severity: 1.6). More recently, in early 2025, SW WA experienced another prolonged, moderate to strong MHW in the region which was also sampled by two glider missions at two critical stages: during the peak (maximum severity: 2.2) and decline (maximum severity: 1.4) of the event, capturing the different phases of the event.

397

These glider observations were critical, not only in validating satellite-derived MHW metrics across regions and seasons, but also in offering detailed subsurface insights beyond satellite capabilities.

400



401

402 **Figure 4. Occurrence and severity of MHWs from January 2009 to June 2025 for (a) Tasmania (TAS), (b) southwest**  
 403 **Western Australia (SW WA), (c) New South Wales (NSW), and (d) Queensland (QLD) with horizontal black lines**  
 404 **indicating periods when glider missions occurred. Light gray bars in 2025 indicate times beyond the study period. MHW**  
 405 **severity values are calculated from selected SST pixels representative of the glider study regions off TAS (148.175° E,**  
 406 **43.125° S), SW WA (115.325° E, 31.625° S), NSW (152.575° E, 32.025° S), and QLD (146.625° E, 17.825° S) .**

407

### 408 3.2 Marine heatwave severity influences on chlorophyll concentrations and dissolved oxygen

409 This section examines the impact of surface MHW severity on both surface and subsurface changes in chlorophyll  
 410 concentrations and dissolved oxygen (DOX) levels from glider-sampled MHWs over the Australian continental  
 411 shelf. Fig. 5 compares chlorophyll and DOX distributions between non-MHW periods and MHW categories  
 412 (moderate and strong), above and below the mixed layer depth (MLD), combining data across all regions. Above  
 413 the MLD, non-MHWs display a broader chlorophyll fluorescence distribution compared to MHWs, whereas below  
 414 the MLD, the probability distributions show minimal variations. DOX, on the other hand, shows distinct shifts in  
 415 probability densities under MHW conditions, with multimodal peaks apparent in both layers, reflecting underlying  
 416 regional and seasonal variations.

417

418 Within the mixed layer, chlorophyll concentrations generally decrease during MHWs (Fig. 5a; thick curves)  
 419 compared to non-MHW conditions. Non-MHW conditions show a peak around  $0.7 \text{ mg m}^{-3}$ , whereas moderate



MHWs peak near  $0.25 \text{ mg m}^{-3}$ , and strong MHWs around  $0.23 \text{ mg m}^{-3}$ , indicating progressively stronger decrease of chlorophyll concentrations in the MLD under increasing MHW severity. Below the MLD, non-MHW conditions show lower subsurface chlorophyll ( $\sim 0.25 \text{ mg m}^{-3}$ ) compared to within the mixed layer, with a slightly more right-skewed distribution (dashed black; Fig. 5c). Moderate MHWs (yellow curve) do not show a significant change in subsurface chlorophyll ( $\sim 0.25 \text{ mg m}^{-3}$ ) from non-MHWs. In contrast, strong MHWs exhibit a peak around  $0.6 \text{ mg m}^{-3}$  (orange curve; Fig. 5c), reflecting elevated subsurface concentrations.

426

For DOX above the MLD, non-MHW periods show a bimodal distribution with the two main peaks at approximately  $180$  and  $220 \text{ } \mu\text{mol kg}^{-1}$ , suggesting the presence of two types of oxygen regimes (Fig. 5b). The first peak near  $220 \text{ } \mu\text{mol kg}^{-1}$  remains stable across non-MHW, moderate and strong severity. Under strong MHWs, the multi-modal structure remains, but the density between  $185\text{--}195 \text{ } \mu\text{mol kg}^{-1}$  is enhanced relative to non-MHW conditions, while density above  $230 \text{ } \mu\text{mol kg}^{-1}$  is reduced. Additionally, a third peak appears near  $165 \text{ } \mu\text{mol kg}^{-1}$  during strong MHWs, which may reflect localized depletion of DOX. These changes indicate that strong MHWs alter the structure of DOX distribution above the MLD, indicating that strong MHWs are associated with a higher frequency of low-oxygen values above the MLD and a relative reduction of high-oxygen values, although the multi-modal structure largely reflects regional and seasonal regimes.

436

For DOX below the MLD (Fig. 5d), the distributions slightly shift toward lower oxygen values under all conditions compared to the layer above. During non-MHW periods, two peaks are observed at approximately  $175$  and  $215 \text{ } \mu\text{mol kg}^{-1}$ . Under moderate MHWs, the distribution collapses into a single dominant peak near  $\sim 205 \text{ } \mu\text{mol kg}^{-1}$ , indicating a homogenization of oxygen conditions below the MLD. Strong MHWs display an elevated lower peak at  $180 \text{ } \mu\text{mol kg}^{-1}$ , similar to above the MLD, and a slightly reduced higher peak around  $205 \text{ } \mu\text{mol kg}^{-1}$ . Overall, the response of DOX to the severity of MHWs appears more heterogeneous and does not follow a uniform leftward shift.

444

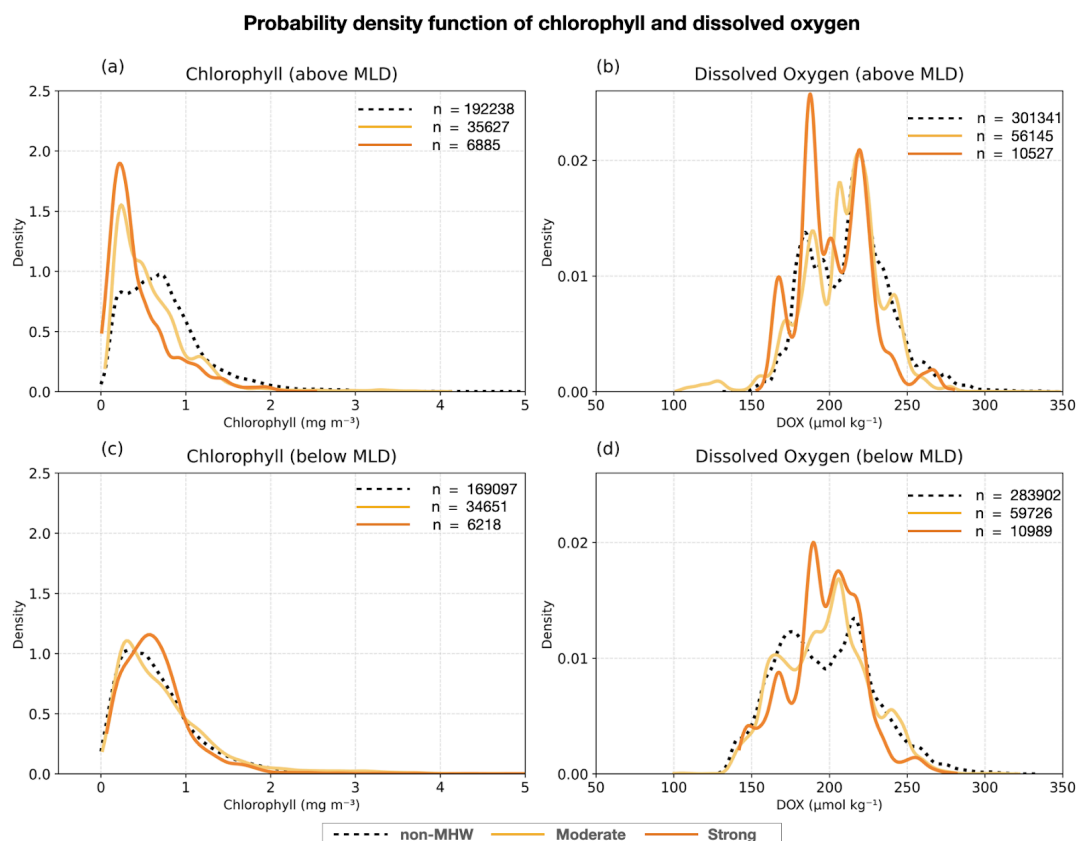
Given that the results combine all regions and seasons, they may mask important regional and seasonal differences, as well as sampling compositions. The following sections analyze the vertical profiles of surface MHWs across study regions and seasons to better understand their subsurface impacts on biogeochemical variables.

448

449

450

451



452

453 Figure 5. Probability density function of (a, c) chlorophyll fluorescence ( $\text{mg m}^{-3}$ ) and (b, d) dissolved oxygen ( $\mu\text{mol kg}^{-1}$ )  
 454 above and below the MLD respectively, during MHWs (thick lines) for all regions. The distribution of chlorophyll and  
 455 dissolved oxygen during MHWs are shown with severity index (S) categories:  $1 < S \leq 2$  (Category 1: moderate; yellow  
 456 curve), and  $2 < S \leq 3$  (Category 2: strong; orange curve), while non-MHW ones are in black ( $S \leq 1$ ; dashed curve). The  
 457 number of samples (n) are indicated.

458

### 459 3.3 Regional and seasonal changes in the water column

460 The vertical temperature structure of surface MHWs provides insight into how these events penetrate below the  
 461 surface and interact with stratification and the mixed layer. These physical changes in the MLD, stratification, and  
 462 MHW depth extent provide the context for examining chlorophyll variations throughout the water column and  
 463 assessing the depth of the DCM in particular seasons and regions. Changes in stratification directly affect  
 464 phytoplankton productivity and oxygen concentrations, making it important to investigate how DOX responds to  
 465 MHWs alongside chlorophyll. In general, DOX is highest at the surface due to diffusion from the atmosphere,



decreasing with depth, and also varies with temperature through solubility. This vertical perspective sets the stage for comparing regional and seasonal patterns, to assess whether chlorophyll and DOX responses to MHWs are consistent across Australia's continental shelf and how they are shaped by local seasonal oceanographic conditions (Figs. 6-9).

### 3.3.1 Eastern Tasmania region: eddy-rich and a convergence zone

Waters off eastern Tasmania (TAS) experience the convergence of warm, salty, and nutrient-poor subtropical waters from the southern extension of the Eastern Australian Current (EAC) and cooler sub-Antarctic waters which lead to complex oceanographic conditions along the continental shelf. The intensification and southward extension of the EAC in the last few decades, associated with changes in the wind stress curl (Hill et al., 2008), has altered stratification and vertical mixing (Holbrook and Bindoff 1997; Ridgway, 2007; Oliver et al., 2017; Chiswell, 2023). These physical changes have implications for biogeochemical processes and overall ecosystem functioning in the region and during MHWs (Chiswell, 2023). From the glider observations, the vertical structure of temperature, salinity, chlorophyll and DOX varied strongly within the seasons (Fig. 6). In the TAS region, glider profiles extended down to about 90 m and showed pronounced seasonal cycles in MLD and MHW depth extent. During summer MHWs, the MLD shoaled to about 18 m in summer (Fig. 6c), shallower than the mean, but extended to the bottom of the water column in winter (Fig. 6a). A similar pattern was reflected in the MHW depth extent, which decreased to about 40 m in summer and deepened to the bottom of the water column in winter. The pronounced seasonality corresponded to variations in stratification, which peaked at about  $7 \times 10^{-3} \text{ s}^{-2}$  near 30 m during summer (Fig. 6k), but was nearly absent in winter (Fig. 6i). Meanwhile, salinity values were consistently higher during MHWs all year round compared to the mean conditions throughout the water column (Figs. 6 e-h), reflecting potential sources of higher saline waters coming onto the shelf from the EAC extension. This indicates that during MHWs, the shelf is influenced by warmer, saltier subtropical water masses associated with a strengthened or southward-shifted EAC, similar to conditions observed during the 2015/2016 Tasman Sea MHW (Oliver et al., 2017). The increased presence of these waters enhances upper-ocean density stratification, particularly in summer, which inhibits vertical mixing with the cooler, fresher sub-Antarctic waters.

Summer MHWs were marked by reduced chlorophyll at the surface relative to the mean in the mixed layer (upper 20 m) but enhanced values at 40 m, exceeding  $1.2 \text{ mg m}^{-3}$  on average (Fig. 6o). During summer, the deepening of the DCM corresponded closely to the MHW depth extent and the depth of maximum stratification. In other seasons, weaker stratification limited the development of strong DCMs both during MHWs and under non-MHWs conditions. The MHW profile of DOX in summer (Fig. 6s) showed a slightly higher concentration in the upper 35 m relative to the mean profile, exceeding 100% saturation within this layer (Fig. S2). This suggests enhanced oxygen production in the mixed layer during MHWs, consistent with the strong DCM, either through photosynthesis, or through mixing (Fig. S2). Similarly, in spring, MHWs showed slightly higher DOX than non-MHW conditions in



the upper 25 m. In contrast, during autumn and winter, DOX during MHWs was consistently lower than the mean conditions throughout the water column due to weak stratification and reduced DCM, or through solubility loss due to warming (Fig. S2), all of which limit phytoplankton productivity and oxygen production.

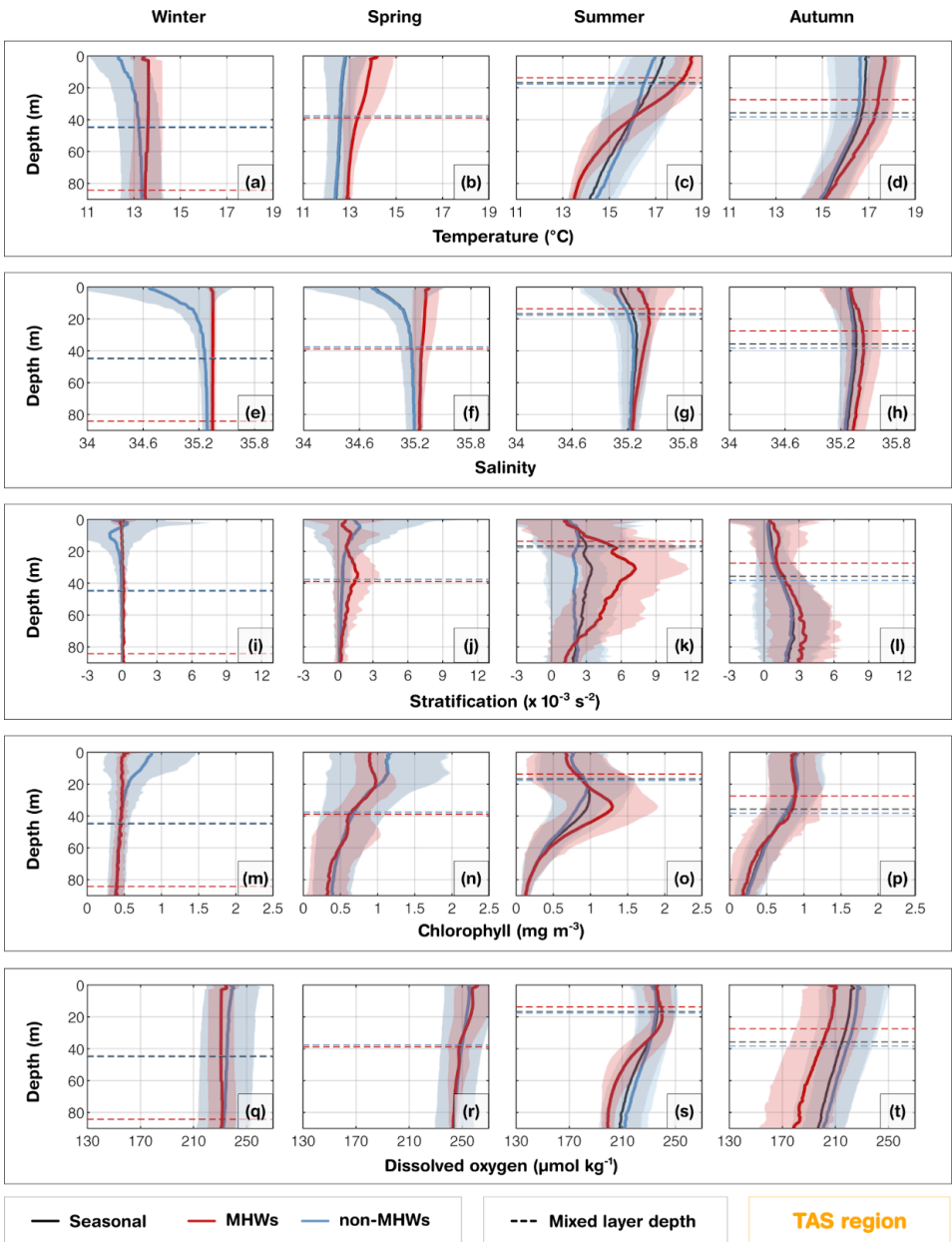




Figure 6. Tasmania region (TAS): Profiles of (a-d) temperature ( $^{\circ}\text{C}$ ), (e-h) salinity (PSU), (i-l) stratification ( $\times 10^{-3} \text{ s}^{-2}$ ), (m-p) chlorophyll ( $\text{mg m}^{-3}$ ) and (q-t) dissolved oxygen ( $\mu\text{mol kg}^{-1}$ ) averaged for all seasonal profiles (black), MHW events (red), and non-MHW events (blue). Horizontal dashed lines are the mean mixed layer depths for the season, MHWs and non-MHWs. Shaded areas represent the respective standard deviations. Seasons are defined as winter (June–August), spring (September–November), summer (December–February), and autumn (March–May).

### 3.3.2 New South Wales region: narrow shelf and boundary current influence

In the New South Wales (NSW) region, the narrow continental shelf waters are shaped by the warm EAC, which contributes to mixing and transports warm nutrient-poor waters onto the shelf when it meanders or shifts inshore. The intrusions of the EAC increases the likelihood of full-depth extended MHWs, which are longer and dominant in winter (Schaeffer et al., 2017, 2023). In this region, seasonal winds and stratification also strongly influence MHWs' depth structure and development, especially in summer (Schaeffer and Roughan, 2017). In the glider observations, during MHWs, warm anomalies were confined to slightly shallower depths ( $\sim 40$  m) in winter compared to austral summer ( $\sim 45$ – $50$  m) and extended deepest in spring ( $\sim 100$  m). Salinity showed no significant change during MHWs and remained relatively stable throughout the water column throughout the year (Figs. 7e–h). Although waters off NSW are generally more stratified in summer than winter, stratification further intensified and deepened during MHWs in all seasons, reaching  $\sim 12 \times 10^{-3} \text{ s}^{-2}$  at 30–40 m in summer and  $\sim 3 \times 10^{-3} \text{ s}^{-2}$  at 45 m in winter, closely matching the depth extent of MHWs (Figs. 7i,k).

The chlorophyll vertical structure and magnitude experienced strong seasonality. Across all seasons, surface chlorophyll concentrations were reduced during MHWs, while increasing at  $\sim 20$ – $40$  m (exceeding  $1 \text{ mg m}^{-3}$ ) during spring and summer (Figs. 7n–o). These chlorophyll maxima were deeper and stronger than under non-MHW conditions, and their depth aligned well with both maximum stratification and the MHW depth extent. In contrast, during autumn and winter, weaker stratification corresponded with shallower or absent DCMs, with chlorophyll concentrations below  $1 \text{ mg m}^{-3}$  (Figs. 7m–p).

In summer, MHWs were associated with reduced DOX in the upper 20 m and below 50 m (Fig. 7s). At intermediate depths, a more pronounced DCM was present (Fig. 7o). However, little difference in DOX levels from non-MHW conditions indicated that photosynthesis was insufficient to alter the total mean DOX (Fig S2). Conversely, in spring, MHWs were associated with higher DOX concentrations in the upper 50 m, exceeding 100% saturation relative to non-MHW conditions within the mixed layer (Fig. S2). This DOX enhancement during spring is consistent with strong stratification and deep DCM (Figs. 7j,n,r), and is likely driven by photosynthesis, mixing or advection of oxygen-rich waters. Moreover, north-eastward winds in spring (Wood et al., 2016), favour downwelling of warmer surface waters, contributing to the deep extent of MHWs in spring (Fig. 7b) and





transporting oxygen to deeper layers. By contrast, in autumn, DOX concentrations were similar within the mixed layer but decreased below the MLD (Fig. 7t; Fig. S2).

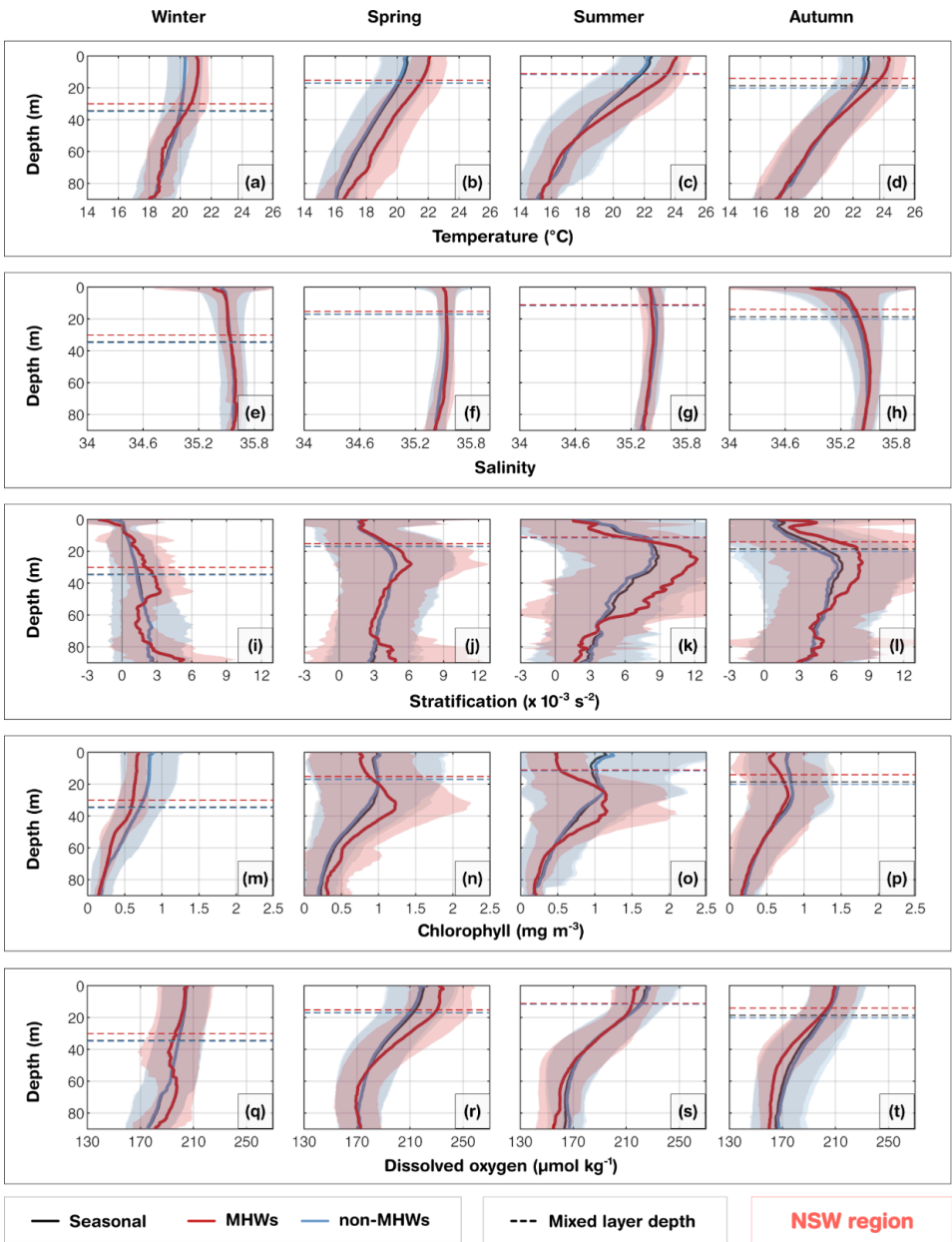


Figure 7. Same as Fig. 6, but for the New South Wales (NSW) region.



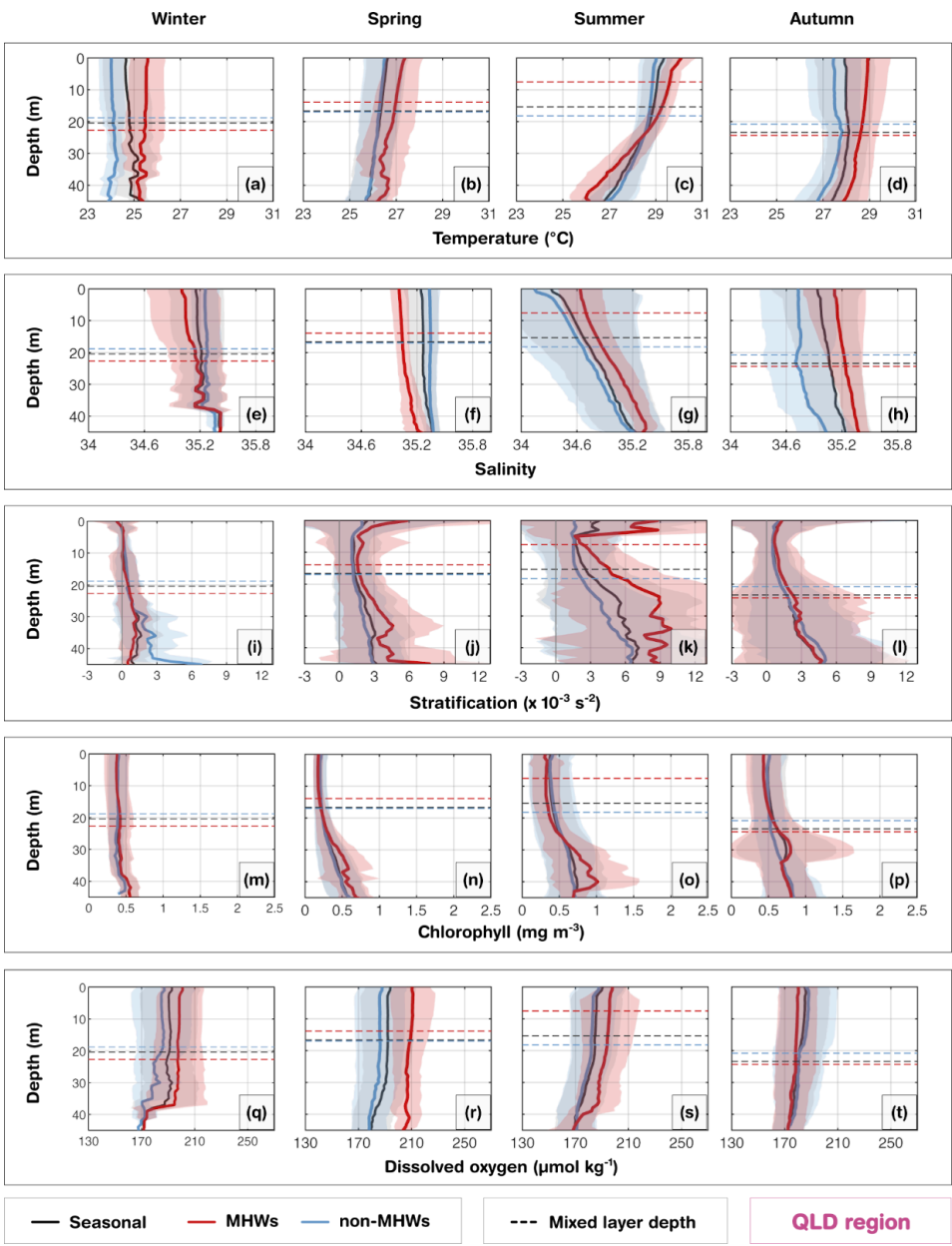
544

### 545 3.3.3 Queensland region: shallow shelf and biologically active

546 The Queensland (QLD) region is home to the Great Barrier Reef, which has a shallow continental shelf with coral  
 547 reefs and reef passages and the shelf circulation is influenced by the Gulf of Papua Current (in the north), East  
 548 Australian Current (EAC; from the central sector to south), the Coral Sea circulation, riverine inputs and  
 549 wind-driven processes (Ridgway et al., 2018; Benthuisen et al., 2022; Wolanski and Kingsford, 2024). The seasonal  
 550 evolution of MLD and the MHW depth extent largely followed the seasonal cycle (Fig. 8). During summer MHWs,  
 551 the MLD shoaled to 9 m, the MHW depth extent reached 25 m, and the stratification peaked above  $10 \times 10^{-3} \text{ s}^{-2}$  at  
 552 35–45 m. This intense near-surface stratification is likely exacerbated by the formation of barrier layers during the  
 553 wet season (Schroeder et al., 2012), where riverine freshwater input and precipitation create a buoyant low-salinity  
 554 lens (Fig. 8g) and subsurface intrusive upwelling through reef passages brings saltier Coral Sea waters below  
 555 (Benthuisen et al. 2016). These barrier layers inhibit vertical mixing, effectively trapping heat in the surface layer  
 556 and intensifying the MHW magnitude. In contrast, during winter MHWs, the MLD deepened to 23 m, the MHW  
 557 depth extent reached about 40 m and stratification weakened to less than  $2 \times 10^{-3} \text{ s}^{-2}$ . The MHW depth extent reached  
 558 deeper depths in both autumn and spring (at least 45 m, which is the depth of our mean profiles), coinciding with  
 559 strong stratification over  $5 \times 10^{-3} \text{ s}^{-2}$  at similar depths. Although fresher waters were observed near the surface in  
 560 winter and spring, salinity values were not as low as in summer, and the vertical salinity gradient was not as  
 561 pronounced as in summer and autumn, suggesting the dominance of wind-driven and convective mixing in  
 562 homogenizing the water column during these cooler seasons.

563

564 Biologically, the strong physical stratification during summer MHWs shaped the vertical chlorophyll structure. The  
 565 DCM reached  $1 \text{ mg m}^{-3}$  at 40 m (Fig. 8o), coinciding with strong fluctuations in stratification levels below 30 m,  
 566 acting as a productive interface where light and nutrient availability overlap. Although less pronounced than  
 567 summer, autumn also displayed high chlorophyll concentrations exceeding  $0.9 \text{ mg m}^{-3}$  at 30 m, suggesting that  
 568 residual stratification and nutrient availability still supported high productivity at depth following the summer bloom  
 569 period. In contrast, winter and spring MHWs showed a weaker coupling between stratification and chlorophyll,  
 570 consistent with enhanced mixing. The DOX during MHWs compared to the mean were consistently higher  
 571 throughout the shallow water column (except in autumn). This presents a thermodynamic anomaly, as warmer water  
 572 typically holds less dissolved gas. Consequently, the observed increase indicates that biological oxygen production  
 573 (photosynthesis) was sufficient to offset the physical solubility loss induced by warming (Fig. S2). While biological  
 574 production dominates the summer signal, the higher DOX observed during MHWs in winter and spring may be  
 575 related to seasonal ventilation that drives the deep vertical extent of temperature anomalies, leading to higher oxygen  
 576 levels than normal. In contrast, the lower DOX levels in autumn, despite the presence of subsurface chlorophyll,  
 577 likely reflect a post-bloom phase where respiration rates increased, consuming oxygen as organic matter from the  
 578 summer bloom remineralized.



579

580 Figure 8. Same as Fig. 6, but for the Queensland (QLD) region.



581

#### 582 3.3.4 Southwest Western Australia region: shallow shelf and oligotrophic conditions

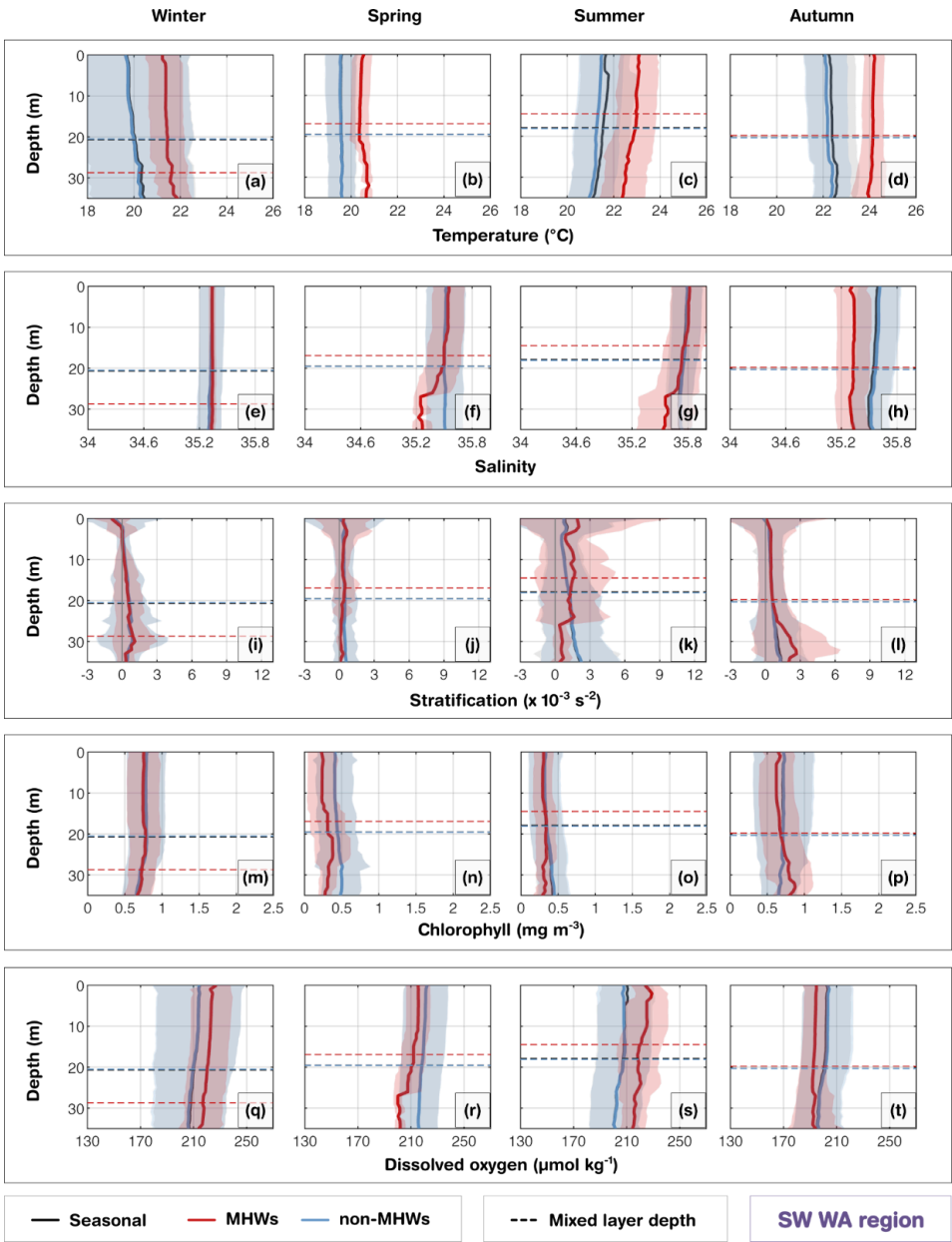
583 The southwest Western Australia (SW WA) region is characterised by a shallow shelf dominated by the warm, fresh  
 584 poleward-flowing Leeuwin Current, maintaining oligotrophic conditions, while the Capes Current emerges inshore  
 585 during spring and summer months with upwelling leading to phytoplankton blooms (Hanson et al., 2005, Feng et al.,  
 586 2025). The gliders sampled over this coastal region, where the shelf narrows from ~50 km to 20 km (Fig. 1e; Brooke  
 587 et al., 2010). From the coast to the mid-shelf, waters had weaker stratification in the upper 40 m (Figs. 9i-j)  
 588 compared with other regions, where the small temperature inversion in autumn and winter is consistent with an  
 589 annual climatology from nearby mooring measurements (Feng et al., 2025). Unlike the stratified systems in eastern  
 590 Australia, this weak stratification coupled with the dominance of the Leeuwin Current drives downwelling-favorable  
 591 conditions that facilitate the rapid vertical propagation of surface heat anomalies. As a result, during surface MHWs,  
 592 anomalously warm surface temperatures extended throughout the depth of our mean profiles (40 m) in all seasons,  
 593 leading to ~+1–2°C differences in the mean temperature profiles compared with non-MHW conditions (Figs. 9a-d).  
 594 The MLD shoaled during MHWs compared to non-MHW conditions, while the MLD was deeper during MHWs in  
 595 winter. In autumn, the MHW conditions were warmer and fresher than non-MHWs, potentially in part related to  
 596 sampling during the 2011 Ningaloo Niño (Fig. 4b), when glider measurements were concentrated around 31.5–32°  
 597 S. During this extreme event, low salinity anomalies were transported by the Leeuwin Current and were some of the  
 598 lowest recorded values since the 1950s (Feng et al., 2015). This highlights that severe MHWs in this region are  
 599 largely advection-driven events, where the transport of buoyant, low-salinity tropical waters enhances the density  
 600 contrast with offshore waters, further trapping heat against the coast.

601

602 Biogeochemically, the strong advective nature of these MHWs exerts a controlling influence on shelf productivity.  
 603 During surface MHWs, shelf waters had lower chlorophyll concentrations during spring (Fig. 9n). Surface MHWs  
 604 were associated with anomalously high DOX during summer and winter reflecting seasonal ventilation (Fig. S2)  
 605 facilitated by the weak stratification, which allows atmospheric oxygen to mix effectively throughout the water  
 606 column. However, significantly lower DOX levels were observed in spring and autumn (Figs. 9r, t). In autumn, with  
 607 sampling through the 2011 Ningaloo Niño, the relatively reduced near-surface chlorophyll and DOX might reflect  
 608 equatorward influences on this region, as offshore waters to the north have been recorded with lower chlorophyll  
 609 and DOX (e.g. Woo and Pattiaratchi, 2008; Weller et al., 2011). This reduction suggests a decoupling from the  
 610 solubility-driven pattern seen in other regions, pointing instead to the physical advection of warm, nutrient-poor, and  
 611 oxygen-depleted tropical waters by the intensified Leeuwin Current, which suppresses local productivity and Capes  
 612 Current upwelling. These results reveal that, in the upper 40 m of coastal waters off SW WA, reduced stratification  
 613 influences the vertical structure of chlorophyll and DOX, even during surface MHWs, and they could be affected by  
 614 latitudinal transport of water properties, as has been found during marine heatwaves caused by a Leeuwin Current  
 615 intensification.



616



617

618 Figure 9. Same as Fig. 6, but for the southwest Western Australia (SW WA) region.

619



#### 620 4. Discussion

621 MHWs have been extensively documented around Australia, yet their impact on subsurface biogeochemical  
622 variables remains a critical gap in our understanding due to limited long-term observations. We used satellite sea  
623 surface temperature and up to 16 years of glider observations across four contrasting and well-observed coastal  
624 regions: eastern Tasmania (TAS), New South Wales (NSW), Queensland (QLD), and southwest Western Australia  
625 (SW WA). Our study reveals how surface MHWs alter, seasonally, the subsurface temperature, stratification, and  
626 biogeochemical variables (chlorophyll and dissolved oxygen). These findings provide new insights into  
627 region-specific responses, which help fill critical gaps in understanding the subsurface impacts of MHWs along the  
628 continental shelf of Australia.

629

630 Each shelf region around Australia has experienced impactful MHWs linked to atmospheric forcing (Schaeffer and  
631 Roughan, 2017; Wang et al., 2023; Gregory et al., 2023; Huang et al., 2024) and regional circulation patterns,  
632 including boundary current intensification. The Tasman Sea has been identified as a global warming hotspot,  
633 experiencing the strongest warming in the Southern Hemisphere (Holbrook and Bindoff, 1997; Hobday and Pecl,  
634 2014); yet biogeochemical data documenting shelf-water responses to MHWs remain scarce. The unprecedented  
635 MHW observed in 2015/16 off Tasmania (captured by a glider mission) led to a wide range of ecological impacts  
636 (Oliver et al., 2017), driven by enhanced eddy kinetic energy associated with a strengthened southward extension of  
637 the East Australian Current (Oliver et al., 2017).

638

639 Off NSW, two glider missions recorded abrupt yet severe MHWs during spring 2013 and 2018, each reaching a  
640 severity index of 3 (based on satellite SST data) and posing severe risks to the shelf ecosystems. MHWs on the  
641 NSW continental shelf have been classified from mooring observations (Schaeffer et al., 2023) as shallow (air-sea  
642 flux driven), extended through the water column (linked to the intrusion of the EAC), or sub-surface only (linked to  
643 downwelling winds). However, these types of MHWs have not been linked to biogeochemical characteristics yet. In  
644 South Australia, the 2013 MHW offers insight into possible impacts in surrounding regions. There, the widespread  
645 MHW triggered harmful algal blooms, resulting in massive fish and abalone mortality, driven by hypoxia and  
646 related physiological stress (Roberts et al., 2019).

647

648 Off QLD, the Great Barrier Reef (GBR), the world's largest coral reef system, has suffered repeated MHW-induced  
649 coral bleaching events, with six mass coral bleaching events between 2016 and 2025 (e.g. Great Barrier Reef Marine  
650 Park Authority et al. 2025). In fact, the event in 2016 was well captured by three glider missions, reaching an MHW  
651 severity index of 2.6 (indicative of strong category). Similarly, the 2020 MHW in the GBR and Coral Sea caused  
652 widespread coral bleaching, with glider missions recording severity values exceeding 2, consistent with observations  
653 reported by Benthuisen et al. (2021). These extreme events were associated with weak wind stress, reduced cloud



cover, and anomalous heat transport (Berkelmans and Oliver, 1999; Schiller et al., 2009; Benthuyssen et al., 2018, 2021).

656

Off SW WA, the shelf is shallow, and the poleward-flowing Leeuwin Current transport warm, nutrient-poor tropical waters southward (Chen et al., 2020), suppressing upwelling and maintaining oligotrophic, vertically homogeneous conditions. The 2011 MHW was triggered by a La Niña–intensified Leeuwin Current (Feng et al., 2013; Benthuyssen et al., 2014), resulting in reduced DOX (Rose et al., 2012), decline in chlorophyll-based productivity (Richardson et al., 2020) and severe ecological and economic consequences (Pearce et al., 2011; Rose et al., 2012). This major MHW (severity index 2.1) was captured by two glider missions (Fig. 4), highlighting the need for continued subsurface MHW monitoring beyond satellite observations.

664

Across most regions, the vertical structure of temperature, salinity, and stratification displayed strong seasonality, with shallow mixed layers and enhanced stratification in summer, and deeper, weaker stratification in winter. During MHWs, these patterns tend to be intensified, with shallower MLD and stronger stratification in summer, and deeper MLD in winter (except in NSW). SW WA exhibited particularly minimal stratification changes due to its naturally well-mixed conditions. The MHW depth extent was shallower in strongly stratified (summer) conditions and deeper during winter when the water column was more homogeneous. These results align with Schaeffer and Roughan (2017), emphasizing the role of stratification and regional hydrography in shaping MHW vertical structure.

672

Chlorophyll responses are tightly coupled to MHW severity and regional hydrography. Results showed that surface chlorophyll above the MLD overall declines with increasing MHW severity, in line with previous studies (Le Grix et al., 2020; Sen Gupta et al., 2020; Gruber et al., 2021) and support the hypothesis that enhanced stratification and reduced nutrient supply from the subsurface limit surface phytoplankton growth during these events. This pattern is evident in the correlation plots (Figs. 10 and S3), which reveal an overall negative relationship between temperature and chlorophyll anomalies above the MLD, except in SW WA where limited sampling may affect the correlation (Fig. S6).

680

Subsurface chlorophyll distributions during MHWs has been a topic of incipient discussion. Here, our study showed evidence for increased chlorophyll below the MLD during strong MHWs along the Australian continental shelves, pointing to the formation of a sharper and deeper DCM in particular seasons. This finding supports hypothesis (2), indicating that despite surface reductions, MHWs can promote deeper chlorophyll maxima and enhanced subsurface productivity. Although the surface becomes nutrient-poor, light still penetrates deeper during MHWs because the MLD becomes shallower, therefore allowing phytoplankton to thrive at depth (e.g. Hayashida and Strutton, 2020). DCM depth correlated strongly with the depth of maximum stratification (Pearson correlation coefficient,  $r = 0.73$  in NSW summer, and  $r = 0.57$  in SW WA autumn; all statistically significant). We also found strong correlations between DCM depth and MHW extent, with the highest values in NSW ( $r = 0.86$  in summer,  $r = 0.70$  in autumn and





690  $r = 0.63$  in spring), followed by significant correlations in TAS ( $r = 0.60$  in summer), and QLD ( $r = 0.60$  in autumn).  
 691 This finding is consistent with Ma and Chen (2025), who showed that MHWs promote DCM development at the  
 692 global scale. In contrast, in winter or in vertically-mixed upper ocean waters such as off SW WA, MHWs penetrate  
 693 to depth, eroding stratification and suppressing DCM. The level of stratification controls the thermocline depth,  
 694 which we found to be strongly correlated with DCM depth (Figs.10 and S5), and thereby governs both the vertical  
 695 position of the DCM and the MHW depth extent. Our results overall suggest that MHW-driven physical changes act  
 696 to redistribute chlorophyll vertically, with regional hydrography (through its influence on stratification) determining  
 697 the extent of it, consistent with hypothesis (4).

698

699 DOX responses to MHW and their severity are less straightforward. Australia's surrounding waters exhibit distinct  
 700 oxygen regimes due to contrasting water masses, biogeochemical environments and seasonal variability.  
 701 Low-oxygen regimes are usually present in tropical and subtropical regions (Paulmier and Ruiz-Pino, 2009; Davila  
 702 et al., 2023) such as QLD and SW WA, influenced by oxygen-poor water masses, while high-oxygen regimes are  
 703 found in temperate regions (NSW, TAS), dominated by well-ventilated waters. During strong MHWs, low-oxygen  
 704 regimes become more oxygenated in the MLD, potentially due to reduced upwelling of oxygen-poor waters under  
 705 shallow MLD. Despite lower nutrients from the subsurface, some regions still can experience enhanced primary  
 706 production due to light availability which in turn increases DOX in the MLD. Besides temperature's direct effect on  
 707 oxygen solubility, changes in DOX arise from complex interactions between circulation and stratification, and  
 708 primary productivity (Gruber, 2011; Gruber et al., 2021).

709

710 Regional differences in DOX distributions during MHWs illustrate these mechanisms. In NSW and TAS, MHWs  
 711 generally decrease DOX in the MLD (except spring NSW, spring and summer TAS), consistent with undersaturated  
 712 conditions (oxygen saturation below 100%; Fig. S2), due to the temperature-dependent decrease in oxygen solubility  
 713 (negative DOX tendency with temperature in Figs. S4a,c). However, below the MLD, localized oxygen increases  
 714 occur particularly in summer, near subsurface chlorophyll maxima (Figs.10, S4b,d). These seasonal increases may  
 715 reflect enhanced biological production during which oxygen is generated below the MLD through photosynthesis, or  
 716 ventilation associated with the strong East Australian Current (EAC) and its eddy-driven intrusions (Malan et al.,  
 717 2020). In addition to these biophysical drivers, regional wind patterns further modulate the vertical structure of DOX  
 718 during spring in NSW. North-eastward winds in spring (Wood et al., 2016), favour downwelling of warmer surface  
 719 waters, contributing to the deeper vertical extent of MHWs and transporting oxygen to subsurface layers.

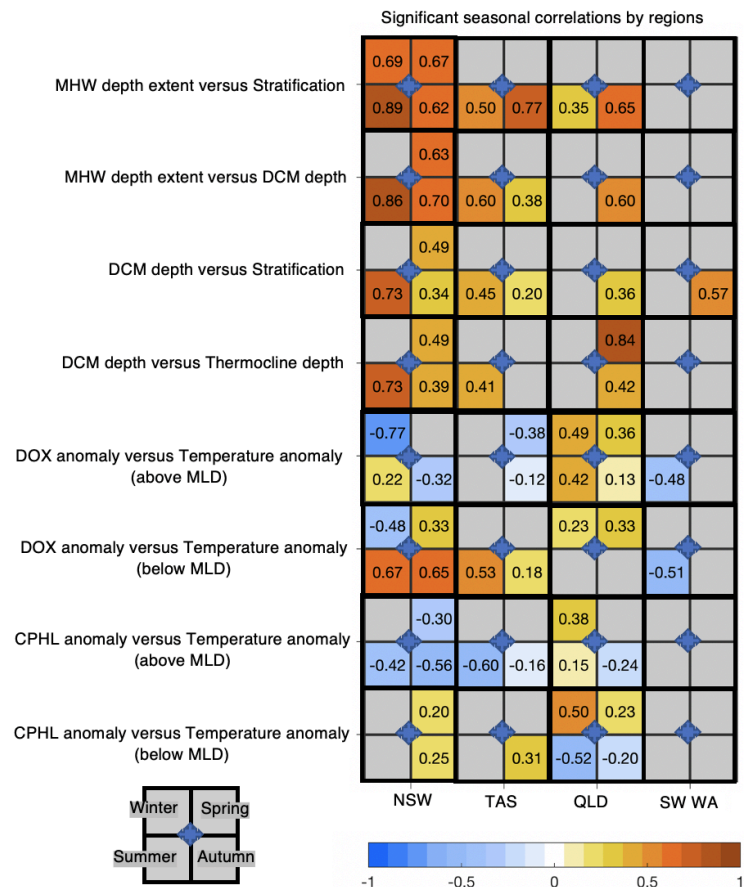
720

721 In QLD, DOX responses to MHWs are linked to seasonal changes in stratification, mixing, and biological  
 722 productivity. During summer MHWs, strong near-surface stratification, reinforced by riverine freshening and  
 723 wet-season rainfall, creates a shallow MLD that traps heat and supports high biological activity. This results in  
 724 elevated DOX throughout the upper water column, with oxygen saturation exceeding 100% in the MLD (Fig. S2),  
 725 indicating that photosynthesis more than compensates for the temperature-driven decline in oxygen solubility. In



contrast, autumn shows lower DOX during MHWs compared to non-MHW periods, although subsurface chlorophyll remains elevated. This reduction coincides with warmer and saltier conditions that decrease oxygen solubility and combined with weaker stratification, facilitates the mixing of low-oxygen waters upward. Enhanced respiration following the summer bloom may also deplete DOX.

In SW WA, well-mixed waters in the upper 40 m exhibited relatively uniform DOX profiles, with enhanced DOX in summer and winter oxygenation during MHWs. For example, in summer, the weakened and offshore-displaced Leeuwin Current combined with strong southerly winds (Feng et al., 2025) promotes strong ventilation and enhanced mixing. During autumn, anomalously warm, fresh waters with reduced chlorophyll in the upper 20 m and reduced DOX, compared with non-MHW conditions, indicate the potential influence for intensified Leeuwin Current transport to affect biogeochemical variables during advection-driven MHWs (Pearce and Feng, 2013). Overall, the study results indicate that stratification and primary productivity jointly regulate oxygen variability, with regional hydrography determining whether MHWs enhance or suppress oxygenation across the water column.



740  
741 Figure 10. Synthesis figure of seasonal correlations between key physical-biogeochemical variables during MHWs across  
742 four regions (NSW, TAS, QLD, SW WA). Rows correspond to variable pairs: (1) MHW depth extent versus stratification,  
743 (2) MHW depth extent versus deep DCM depth, (3) DCM depth versus stratification, (4) DCM depth versus thermocline  
744 depth, (5) dissolved oxygen anomalies (DOX) versus temperature anomalies (above the MLD), (6) dissolved oxygen  
745 anomalies (DOX) versus temperature anomalies (below the MLD); (7) chlorophyll anomalies versus temperature  
746 anomalies (in the MLD); and (8) chlorophyll anomalies versus temperature anomalies (below the MLD). Columns  
747 correspond to regions. Each cell is subdivided into four seasonal quadrants, colored by the Pearson correlation  
748 (r) values with values indicated within each quadrant.  
749

750 5. Conclusions

751 This study shows that the impacts of MHWs on dissolved oxygen and chlorophyll along the Australian continental  
752 shelf depend strongly on regional hydrography, seasonal stratification, and, to some extent, event severity. Taken



753 together, our results show that surface-only perspectives underestimate the biogeochemical and potential ecological  
754 impacts of MHWs. Subsurface glider observations revealed that MHWs can simultaneously suppress surface  
755 productivity while intensifying subsurface production, with consequences for oxygen levels and food-web  
756 dynamics, depending on regional hydrography and stratification. Stratification, which appears consistently enhanced  
757 during summer MHWs, emerges as a useful proxy for the vertical extent of surface MHWs and on the DCM. These  
758 findings underscore the importance of accounting for region-specific monitoring to manage ecological consequences  
759 of MHWs.

760

761 The interaction between physical processes, such as seasonal circulation, stratification and biological feedback,  
762 including deep chlorophyll maxima formation and oxygen production, highlights the complex biogeochemical  
763 responses to MHWs. By leveraging up to 16 years of glider observations, this work demonstrates the importance of  
764 sustained subsurface monitoring and coupled physical–biogeochemical approaches to better predict ecosystem  
765 vulnerability. Future research is needed to transform sparse and high-frequency sampling of continental shelf waters  
766 to develop coastal climatologies appropriate for assessing subsurface marine heatwave impacts. Long-term  
767 measurements are key to improving our understanding of MHWs’ vertical structure, drivers, and ecological  
768 consequences and, in combination with shelf modelling, can provide a holistic view of how they affect variability  
769 and extremes in our coastal and shelf systems. These efforts are critical for managing the impacts of MHWs on  
770 marine ecosystems under a warming climate.

771

772 **Data availability:** The glider data is publicly available through the Australian Ocean Data Network (AODN) Portal  
773 at: <https://portal.aodn.org.au/search?uuid=c317b0fe-02e8-4ff9-96c9-563fd58e82ac> and  
774 <https://thredds.aodn.org.au/thredds/catalog/IMOS/ANFOG/catalog.html>.

775 The NOAA CoralTemp v3.1 SST product is available at: <https://coralreefwatch.noaa.gov/product/5km/index.php>.

776 The IMOS OceanCurrent delayed-mode, gridded (adjusted) sea level anomaly product and surface geostrophic  
777 velocity is available from 1993–2020 at:

778 <https://thredds.aodn.org.au/thredds/catalog/IMOS/OceanCurrent/GSLA/DM/catalog.html>, while the near-real-time  
779 data is available at: <https://thredds.aodn.org.au/thredds/catalog/IMOS/OceanCurrent/GSLA/NRT/catalog.html>.

780 **Code availability:** The code will be available at the time of publication on Github.

781 **Author contributions:** DM lead the project in assigning analysis and writing. JA and RLG assisted with data  
782 reprocessing. AS designed and supervised the project. All authors contributed to the analyses, discussions, writing  
783 and proofreading.

784 **Competing interests:** The authors declare that they have no conflict of interest.



**785 Acknowledgments:** We would like to acknowledge CLIVAR (Climate and Ocean – Variability, Predictability and  
 786 Change) 2023 Marine heatwave summer school, through which this project started. We also thank everyone who  
 787 was involved in the glider deployment, piloting, and processing, through the IMOS Ocean Gliders Facility led by  
 788 Prof. Charitha Pattiaratchi, as well as the IMOS Event Based Sampling national committee. All glider data were  
 789 sourced from Australia’s Integrated Marine Observing System (IMOS) – IMOS is enabled by the National  
 790 Collaborative Research Infrastructure Strategy (NCRIS). It is operated by a consortium of institutions as an  
 791 unincorporated joint venture, with the University of Tasmania as Lead Agent.

**792 Financial support:**

793

794 FEKG. acknowledges funding from Canada’s C150 Research Program (Grant No. 50296) and Schmidt Sciences,  
 795 LLC.

796

**797 References**

- 798 Amaya, D. J., Miller, A. J., Xie, S.-P., and Kosaka, Y.: Physical drivers of the summer 2019 North Pacific marine  
 799 heatwave, *Nat. Commun.*, 11(1), 1903, doi:10.1038/s41467-020-15820-w, 2020
- 800 Benthuisen, J., Feng, M., and Zhong L.: Spatial patterns of warming off Western Australia during the 2011  
 801 Ningaloo Niño: Quantifying impacts of remote and local forcing, *Cont. Shelf Res.*, 91, 232-246,  
 802 doi:10.1016/j.csr.2014.09.014, 2014.
- 803 Benthuisen, J. A., Tonin, H., Brinkman, R., Herzfeld, M., and Steinberg, C.: Intrusive upwelling in the Central  
 804 Great Barrier Reef. *J. of Geophys. Res.: Oceans*, 121(11), pp.8395-8416, doi:10.1002/2016JC012294, 2016.
- 805 Benthuisen, J. A., Oliver, E. C. J., Feng, M., and Marshall, A. G.: Extreme marine warming across tropical Australia  
 806 during austral summer 2015–2016, *J. Geophys. Res.: Oceans*, 123(2), 1301-1326, doi:10.1002/2017JC013326,  
 807 2018.
- 808 Benthuisen, J. A., Steinberg, C., Spillman, C. M., and Smith, G. A.: Oceanographic drivers of bleaching in the  
 809 GBR: from observations to prediction. Volume 4: Observations and predictions of marine heatwaves. Report to  
 810 the National Environmental Science Program. Reef and Rainforest Research Centre Limited, Cairns (47pp.).  
 811 Available at: <https://nesptropical.edu.au/index.php/round-4-projects/project-4-2/>, 2021.
- 812 Benthuisen, J. A., Emslie, M. J., Currey-Randall, L. M., Cheal, A. J. and Heupel, M. R.: Oceanographic influences  
 813 on reef fish assemblages along the Great Barrier Reef, *Prog. Oceanogr.*, 208, p.102901,  
 814 doi:10.1016/j.pocean.2022.102901, 2022.
- 815 Benthuisen, J. A., Pattiaratchi, C., Spillman, C. M., Govekar, P., Beggs, H., Bastos de Oliveira, H., Chandrapavan,  
 816 A., Feng, M., Hobday, A. J., Holbrook, N. J., Jaine, F. R. A., and Schaeffer, A.: Observing marine heatwaves  
 817 using ocean gliders to address ecosystem challenges through a coordinated national program. In *Frontiers in*  
 818 *Ocean Observing*. E.S. Kappel, V. Cullen, I.C.A. da Silveira, G. Coward, C. Edwards, P. Heimbach, T. Morris,  
 819 H. Pillar, M. Roughan, and J. Wilkin, eds, *Oceanogr.* 38(Supplement 1), doi:10.5670/oceanog.2025e101, 2025.



- 820 Berkelmans, R., & Oliver, J. K.: Large-scale bleaching of corals on the Great Barrier Reef. *Coral reefs*, 18(1), 55–60,  
 821 doi:10.1007/s003380050154, 1999.
- 822 Blondeau-Patissier, D., Gower, J. F. R., Dekker, A. G., Phinn, S. R., and Brando, V. E.: A review of ocean color  
 823 remote sensing methods and statistical techniques for the detection, mapping and analysis of phytoplankton  
 824 blooms in coastal and open oceans, *Prog. Oceanogr.*, 123, 123–144, doi:10.1016/j.pocean.2013.12.008, 2014.
- 825 Brooke, B., Creasey, J., and Sexton, M.: Broad-scale geomorphology and benthic habitats of the Perth coastal plain  
 826 and Rottnest Shelf, Western Australia, identified in a merged topographic and bathymetric digital relief model,  
 827 *Intern. J. Rem. Sens.*, 31(23), 6223–6237, doi: 10.1080/01431160903403052, 2010.
- 828 Capotondi, A., Rodrigues, R. R., Sen Gupta, A., Benthuisen, J. A., Deser, C., Frölicher, T. L., Lovenduski, N. S.,  
 829 Amaya, D. J., Le Grix, N., Xu, T., and Hermes, J.: A global overview of marine heatwaves in a changing climate,  
 830 *Commun. Earth Environ.*, 5, 701, doi:10.1038/s43247-024-01806-9, 2024.
- 831 Cavole, L. M., Demko, A. M., Diner, R. E., Giddings, A., Koester, I., Pagniello, C. M., ... and Franks, P. J.:  
 832 Biological impacts of the 2013–2015 warm-water anomaly in the Northeast Pacific: winners, losers, and the  
 833 future, *Oceanogr.*, 29(2), 273–285. doi:10.5670/oceanog.2016.32, 2016.
- 834 Chen, M., Pattiaratchi, C. B., Ghadouani, A., and Hanson, C.: Seasonal and inter-annual variability of water column  
 835 properties along the Rottnest continental shelf, south-west Australia, *Ocean Sci.*, 15, 333–348,  
 836 doi:10.5194/os-15-333-2019, 2019.
- 837 Chen, M., Pattiaratchi, C. B., Ghadouani, A. and Hanson C.: Influence of storm events on chlorophyll distribution  
 838 along the oligotrophic continental shelf off south-western Australia, *Front. Mar. Sci.*, 7, 287,  
 839 doi:10.3389/fmars.2020.00287, 2020.
- 840 Chen, Q., Li, D., Feng, J., Zhao, L., Qi, J., and Yin, B.: Understanding the compound marine heatwave and  
 841 low-chlorophyll extremes in the western Pacific Ocean, *Front. Mar. Sci.*, 10, 1303663,  
 842 doi:10.3389/fmars.2023.1303663, 2023.
- 843 Chiswell, S. M.: Tasman Sea high- and low- chlorophyll events, their links to marine heat waves, cool spells, and  
 844 global teleconnections, *New Zealand J. Mar. Fresh. Res.*, 57(4), 550–567, doi:10.1080/00288330.2022.2076702,  
 845 2023.
- 846 Davila, X., Olsen, A., Lauvset, S. K., McDonagh, E. L., Brakstad, A., and Gebbie, G.: On the origins of open ocean  
 847 oxygen minimum zones, *J. Geophys. Res.: Oceans*, 128(8), e2023JC019677, doi:10.1029/2023JC019677, 2023.
- 848 Davies, K. T.: Using passive acoustic monitoring from gliders for near realtime detection and dynamic management  
 849 of North Atlantic right whales (*Eubalaena glacialis*) in the Laurentian Channel Dynamic Shipping Zones, 2021.
- 850 Eakins, B. W., and Sharman, G. F. (2010). Volumes of the World's Oceans from ETOPO1. NOAA National  
 851 Geophysical Data Center, Boulder, CO, 7(1).
- 852 Feng, M., McPhaden, M. J., Xie, S.-P., and Hafner, J.: La Niña forces unprecedented Leeuwin Current warming in  
 853 2011, *Sci. Rep.*, 3(1), 1277, doi:10.1038/srep01277, 2013.



- 854 Feng, M., Benthuisen, J., Zhang, N., and Slawinski, D.: Freshening anomalies in the Indonesian throughflow and  
 855 impacts on the Leeuwin Current during 2010–2011, *Geophys. Res. Lett.*, 42(20), 8555–8562,  
 856 doi:10.1002/2015GL065848, 2015.
- 857 Feng, M., Caputi, N., Chandrapavan, A., Chen, M., Hart, A., and Kangas, M.: Multi-year marine cold-spells off the  
 858 west coast of Australia and effects on fisheries, *J. Mar. Sys.*, 214, 103473, doi:10.1016/j.jmarsys.2020.103473,  
 859 2021.
- 860 Feng, M., Bui, T., and Benthuisen, J. A.: Seasonal climatology of the Leeuwin Current-Capes Current system off  
 861 southwest Australia from long-term moored observations, *J. Geophys. Res.: Oceans*, 130(5), e2025JC022662,  
 862 doi:10.1029/2025JC022662, 2025.
- 863 Frölicher, T. L., Fischer, E. M. and Gruber, N.: Marine heatwaves under global warming, *Nature*, 560, 360–364,  
 864 doi:10.1038/S31586-018-0383-9, 2018.
- 865 Garcia, H. E., & Gordon, L. I.: Oxygen solubility in seawater: Better fitting equations. *Limnology and*  
 866 *oceanography*, 37(6), 1307–1312, doi:10.4319/lo.1992.37.6.1307, 1992.
- 867 Gomes, D. G., Ruzicka, J. J., Crozier, L. G., Huff, D. D., Brodeur, R. D., and Stewart, J. D.: Marine heatwaves  
 868 disrupt ecosystem structure and function via altered food webs and energy flux. *Nat. Commun.*, 15(1), 1988.  
 869 doi:10.1038/s41467-024-46263-2, 2024.
- 870 Great Barrier Reef Marine Park Authority, Australian Institute of Marine Science, and CSIRO.: Reef Snapshot:  
 871 Summer 2024–25, Reef Authority, Townsville, Available at: <https://hdl.handle.net/11017/4116>, 2025.
- 872 Gregory, C. H., Holbrook, N. J., Marshall, A. G., and Spillman, C. M.: Atmospheric drivers of Tasman Sea marine  
 873 heatwaves, *J. Climate*, 36(15), 5197–5214, doi:10.1175/JCLI-D-22-0538.1, 2023.
- 874 Gruber, N.: Warming up, turning sour, losing breath: ocean biogeochemistry under global change, *Phil. Trans. R.*  
 875 *Soc. A.*, 3691980, doi:10.1098/rsta.2011.0003, 2011.
- 876 Gruber, N., Boyd, P. W., Frölicher, T. L., and Vogt, M.: Biogeochemical extremes and compound events in the  
 877 ocean, *Nature*, 600, 395–407, doi:10.1038/s41586-021-03981-7, 2021.
- 878 Hanson, C. E., Pattiaratchi, C. B., and Waite, A. M.: Sporadic upwelling on a downwelling coast: phytoplankton  
 879 responses to spatially variable nutrient dynamics off the Gascoyne region of Western Australia, *Cont. Shelf Res.*,  
 880 25(12–13), 1561–1582, doi:10.1016/j.csr.2005.04.003, 2005.
- 881 Hayashida, H., Matear, R. J., and Strutton, P. G.: Background nutrient concentration determines phytoplankton  
 882 bloom response to marine heatwaves, *Glob. Change Bio.*, 26(9), 4800–4811, doi:10.1111/gcb.15255, 2020.
- 883 Hill, K. L., Rintoul, S. R., Coleman, R., and Ridgway, K. R.: Wind forced low frequency variability of the East  
 884 Australia Current, *Geophys. Res. Lett.*, 35(8), doi:10.1029/2007GL032912, 2008.
- 885 Hobday, A. J., & Pecl, G. T.: Identification of global marine hotspots: sentinels for change and vanguards for  
 886 adaptation action. *Reviews in Fish Biology and Fisheries*, 24(2), 415–425, doi:10.1007/s11160-013-9326-6,  
 887 2014.





- 888 Hobday, A. J., Alexander, L. V., Perkins, S. E., Smale, D. A., Straub, S. C., Oliver, E. C. J., Benthuisen, J. A.,  
 889 Burrows, M. T., Donat, M. G., Feng, M., and Holbrook, N. J.: A hierarchical approach to defining marine  
 890 heatwaves, *Prog. Oceanogr.*, 141, 227-238, doi:10.1016/j.pocean.2015.12.014, 2016.
- 891 Hobday, A. J., Oliver, E. C., Sen Gupta, A., Benthuisen, J. A., Burrows, M. T., Donat, M. G., ... and Smale, D. A.:  
 892 Categorizing and naming marine heatwaves, *Oceanogr.*, 31(2), 162-173, doi:10.5670/oceanog.2018.205, 2018.
- 893 Holbrook, N. J., and Bindoff, N. L.: Interannual and decadal temperature variability in the southwest Pacific Ocean  
 894 between 1955 and 1988, *J. Clim.*, 10(5), 1035-1049.  
 895 doi:10.1175/1520-0442(1997)010<1035:IADTVI>2.0.CO;2, 1997.
- 896 Holbrook, N. J., Hernaman, V., Koshiba, S., Lako, J., Kajtar, J. B., Amosa, P., and Singh, A.: Impacts of marine  
 897 heatwaves on tropical western and central Pacific Island nations and their communities, *Global and Planetary*  
 898 *Change*, 208, 103680, doi.org/10.1016/j.gloplacha.2021.103680, 2022.
- 899 Huang, Z., Feng, M., Dalton, S. J., and Carroll, A. G.: Marine heatwaves in the Great Barrier Reef and Coral Sea:  
 900 their mechanisms and impacts on shallow and mesophotic coral ecosystems, *Sci. Total Env.*, 908, 168063,  
 901 doi:10.1016/j.scitotenv.2023.168063, 2024.
- 902 IMOS 2025, “OceanCurrent - Gridded sea level anomaly - Delayed mode - DM02”,  
 903 [https://catalogue-imos.aodn.org.au/geonetwork/srv/eng/catalog.search#/metadata/da30c0b8-4978-4a26-915e-b80](https://catalogue-imos.aodn.org.au/geonetwork/srv/eng/catalog.search#/metadata/da30c0b8-4978-4a26-915e-b80c88bb4510)  
 904 [c88bb4510](https://catalogue-imos.aodn.org.au/geonetwork/srv/eng/catalog.search#/metadata/da30c0b8-4978-4a26-915e-b80c88bb4510), accessed August-2025.
- 905 Kwiatkowski, L., Torres, O., Bopp, L., Aumont, O., Chamberlain, M., Christian, J. R., ... & Ziehn, T.: Twenty-first  
 906 century ocean warming, acidification, deoxygenation, and upper-ocean nutrient and primary production decline  
 907 from CMIP6 model projections. *Biogeosciences*, 17(13), 3439-3470, doi:10.5194/bg-17-3439-2020, 2020.
- 908 Lachkar, Z., Lévy, M., and Smith, K. S.: Strong intensification of the Arabian Sea oxygen minimum zone in  
 909 response to Arabian Gulf warming. *Geophys. Res. Lett.*, 46(10), 5420–5429, doi:10.1029/2018GL081631, 2019.
- 910 Laufkötter, C., Zscheischler, J., and Frölicher, T. L.: High-impact marine heatwaves attributable to human-induced  
 911 global warming, *Science*, 369(6511), 1621–1625. doi:10.1126/science.aba0690, 2020.
- 912 Le Gendre, R., Varillon, D., Fiat, S., Hocdé, R., de Ramon N'Yeurt, A., Andréfouët, S., ... & Menkes, C.:  
 913 ReefTEMPS: the Pacific Islands coastal temperature network. *Earth System Science Data*, 17(10), 5277-5301,  
 914 doi:10.5194/essd-17-5277-202510.5194/essd-17-5277-2025, 2025.
- 915 Le Grix, N., Zscheischler, J., Laufkötter, C., Rousseaux, C. S., and Frölicher, T. L.: Compound high temperature and  
 916 low chlorophyll extremes in the ocean over the satellite period, *Biogeosci. Discussions*, 2020, 1-26.  
 917 doi:10.5194/bg-18-2119-2021, 2020.
- 918 Ma, X. and Chen, G.: Marine heatwaves are shaping the vertical structure of phytoplankton in the global ocean.  
 919 *Commun. Earth Environ.*, 6, 715, doi:10.1038/S33247-025-02718-y, 2025.
- 920 Malan, N., Archer, M., Roughan, M., Cetina-Heredia, P., Hemming, M., Rocha, C., ... and Queiroz, E.: Eddy-driven  
 921 cross-shelf transport in the East Australian Current separation zone, *J. Geophys. Res.: Oceans*, 125(2),  
 922 e2019JC015613, doi: 10.1029/2019JC015613, 2020.



- 923 Malan, N., Sen Gupta, A., Schaeffer, A., Zhang, S., Doblin, M. A., Pilo, G. S., ... and Spillman, C. M.: Lifting the lid  
 924 on marine heatwaves, *Prog. Oceanogr.*, 103539, doi:10.1016/j.pocean.2025.103539, 2025.
- 925 Marre, J. B., Thebaud, O., Pascoe, S., Jennings, S., Boncoeur, J., and Coglean, L.: The use of ecosystem services  
 926 valuation in Australian coastal zone management, *Marine Policy*, 56, 117-124,  
 927 doi:10.1016/j.marpol.2015.02.011, 2015.
- 928 Meier, H. M., Väli, G., Naumann, M., Eilola, K., and Frauen, C.: Recently accelerated oxygen consumption rates  
 929 amplify deoxygenation in the Baltic Sea, *J. Geophys. Res.: Oceans*, 123(5), 3227-3240,  
 930 doi:10.1029/2017JC013686, 2018.
- 931 Noh, K. M., Lim, H. G., and Kug, J. S.: Global chlorophyll responses to marine heatwaves in satellite ocean color.  
 932 *Environ. Res. Lett.*, 17(6), 064034, doi:10.1088/1748-9326/ac70ec, 2022.
- 933 Oliver, E. C., Benthuisen, J. A., Bindoff, N. L., Hobday, A. J., Holbrook, N. J., Mundy, C. N., and  
 934 Perkins-Kirkpatrick, S. E.: The unprecedented 2015/16 Tasman Sea marine heatwave, *Nat. Commun.*, 8(1),  
 935 16101, doi:10.1038/ncomms16101, 2017.
- 936 Oliver, E. C., Benthuisen, J. A., Darmaraki, S., Donat, M. G., Hobday, A. J., Holbrook, N. J., ... and Sen Gupta, A.:  
 937 Marine heatwaves, *Ann. Rev. Mar. Sci.*, 13(1), 313-342, doi:10.1146/annurev-marine-032720-095144, 2021.
- 938 Pattiaratchi, C., Hollings, B., Woo, M., and Welhena, T.: Dense shelf water formation along the south-west  
 939 Australian inner shelf, *Geophys. Res. Lett.*, 38, L10609, doi:10.1029/2011GL046816, 2011.
- 940 Pattiaratchi, C., Woo, L. M., Thomson, P. G., Hong, K. K., and Stanley, D.: Ocean glider observations around  
 941 Australia. *Oceanogr.*, 30(2), 90-91, doi:10.5670/oceanog.2017.226, 2017.
- 942 Paulmier, A. and Ruiz-Pino, D.: Oxygen minimum zones (OMZs) in the modern ocean.: *Prog. Oceanogr.*, 80(3-4),  
 943 113-128, doi:10.1016/j.pocean.2008.08.001, 2009.
- 944 Pearce, A., Lenanton, R., Jackson, G., Moore, J., Feng, M., and Gaughan, D.: The “marine heat wave” off Western  
 945 Australia during the summer of 2010/11, Fisheries Research Report No. 222, Department of Fisheries, Western  
 946 Australia. 40pp., Available at: [https://www.fish.wa.gov.au/documents/research\\_reports/frr222.pdf](https://www.fish.wa.gov.au/documents/research_reports/frr222.pdf), 2011.
- 947 Pearce, A. F. and Feng, M.: The rise and fall of the “marine heat wave” off Western Australia during the summer of  
 948 2010/2011, *J. Mar. Sys.*, 111, 139-156, doi:10.1016/j.jmarsys.2012.10.009, 2013.
- 949 Richardson, A. J., Savage, J., Coman, F., Davies, C., Eriksen, R., McEnnulty, F., Slotwinski, A., Tonks, M.,  
 950 Uribe-Palomino, J.: The impact on zooplankton of the 2011 heatwave off Western Australia. In Richardson, A.  
 951 J., Eriksen, R., Moltmann, T., Hodgson-Johnston, I., Wallis, J. R. (Eds). State and trends of Australia’s ocean  
 952 Report, doi:10.26198/5e16adc449e87, 2020.
- 953 Ridgway, K. R.: Long-term trend and decadal variability of the southward penetration of the East Australian  
 954 Current, *Geophys. Res. Lett.*, 34(13), doi:10.1029/2007GL030393, 2007.
- 955 Ridgway, K. R., Benthuisen, J. A., and Steinberg, C.: Closing the gap between the Coral Sea and the equator: Direct  
 956 observations of the north Australian western boundary currents, *J. Geophys. Res.: Oceans*, 123(12), 9212-9231,  
 957 doi:10.1029/2018JC014269, 2018.



- 958 Ridgway, K. R. and Ling, S. D.: Three decades of variability and warming of nearshore waters around Tasmania,  
 959 Prog. Oceanogr., 215, 103046, doi:10.1016/j.pocean.2023.103046, 2023.
- 960 Roberts, S. D., Van Ruth, P. D., Wilkinson, C., Bastianello, S. S., & Bansemer, M. S.: Marine heatwave, harmful  
 961 algae blooms and an extensive fish kill event during 2013 in South Australia. *Frontiers in Marine Science*, 6,  
 962 610, doi:10.3389/fmars.2019.00610, 2019.
- 963 Rose, T. H., Smale, D. A., and Botting, G.: The 2011 marine heat wave in Cockburn Sound, southwest Australia.  
 964 Ocean Sci., 8(4), 545-550, doi:10.5194/os-8-545-2012, 2012.
- 965 Rudnick, D. L.: Ocean research enabled by underwater gliders, *Ann. Rev. Mar. Sci.*, 8(1), 519-541,  
 966 doi:10.1146/annurev-marine-122414-033913, 2016.
- 967 Safonova, K., Meier, H. M., and Gröger, M.: Summer heatwaves on the Baltic Sea seabed contribute to oxygen  
 968 deficiency in shallow areas, *Comm. Earth Environ.*, 5(1), 106, doi:10.1038/s43247-024-01268-z, 2024.
- 969 Sampaio, E., Santos, C., Rosa, I. C., Ferreira, V., Pörtner, H.-O., Duarte, C. M., Levin, L. A., and Rosa, R.: Impacts  
 970 of hypoxic events surpass those of future ocean warming and acidification, *Nat. Ecol. Evol.*, 5(3), 311-321,  
 971 doi:10.1038/s41559-020-01370-3, 2021.
- 972 Schaeffer, A., Roughan, M., & Wood, J. E.: Observed bottom boundary layer transport and uplift on the continental  
 973 shelf adjacent to a western boundary current. *Journal of Geophysical Research: Oceans*, 119(8), 4922-4939,  
 974 doi:10.1002/2013JC009735, 2014.
- 975 Schaeffer, A., Roughan, M., Jones, E. M., and White, D.: Physical and biogeochemical spatial scales of  
 976 variability in the East Australian Current separation from shelf glider measurements, *Biogeosciences*, 13,  
 977 1967–1975, doi:10.5194/bg-13-1967-2016, 2016a.
- 978 Schaeffer, A., Roughan, M., Austin, T., Everett, J. D., Griffin, D., Hollings, B., ... and White, D.: Mean  
 979 hydrography on the continental shelf from 26 repeat glider deployments along southeastern Australia, *Sci. Data*,  
 980 3(1), 1-12, doi:10.1038/sdata.2016.70, 2016b.
- 981 Schaeffer, A., and Roughan, M.: Subsurface intensification of marine heatwaves off southeastern Australia: The role  
 982 of stratification and local winds, *Geophys. Res. Lett.*, 44(10), 5025-5033, doi:10.1002/2017GL073714, 2017.
- 983 Schaeffer, A., Sen Gupta, A., and Roughan, M.: Seasonal stratification and complex local dynamics control the  
 984 sub-surface structure of marine heatwaves in Eastern Australian coastal waters, *Commun. Earth Environ.*, 4(1),  
 985 304, doi: 10.1038/s43247-023-00966-4, 2023.
- 986 Schiller, A., Ridgway, K. R., Steinberg, C. R., and Oke, P. R.: Dynamics of three anomalous SST events in the Coral  
 987 Sea, *Geophys. Res. Lett.*, 36(6), doi:10.1029/2008GL036997, 2009.
- 988 Schroeder, T., Devlin, M. J., Brando, V. E., Dekker, A. G., Brodie, J. E., Clementson, L. A., & McKinna, L.:  
 989 Inter-annual variability of wet season freshwater plume extent into the Great Barrier Reef lagoon based on  
 990 satellite coastal ocean colour observations. *Marine Pollution Bulletin*, 65(4–9), 210–223,  
 991 doi:10.1016/j.marpolbul.2012.02.022, 2012.



- 992 Sen Gupta, A., Thomsen, M., Benthuyssen, J. A., Hobday, A. J., Oliver, E., Alexander, L. V., ... and Smale, D. A.:  
 993 Drivers and impacts of the most extreme marine heatwave events, *Sci. Rep.*, 10,  
 994 doi:10.1038/S31598-020-75445-3, 2020.
- 995 Siefert, R. L. and Plattner, G.-K.: The role of coastal zones in global biogeochemical cycles, *Eos Trans. AGU*,  
 996 85(45), 470-470, doi:10.1029/2004EO450005, 2004.
- 997 Skirving, W., Marsh, B., De La Cour, J., Liu, G., Harris, A., Maturi, E., ... and Eakin, C. M.: CoralTemp and the  
 998 Coral Reef Watch coral bleaching heat stress product suite version 3.1, *Rem. Sens.*, 12(23), 3856,  
 999 doi:10.3390/rs12233856, 2020.
- 1000 Smith, K. E., Burrows, M. T., Hobday, A. J., King, N. G., Moore, P. J., Sen Gupta, A., Moore, P. J., Thomsen, M.,  
 1001 Wernberg, T., and Smale, D. A.: Socioeconomic impacts of marine heatwaves: Global issues and opportunities,  
 1002 *Science*, 374, eabj3593, doi:10.1126/science.abj3593, 2021.
- 1003 Smith, K. E., Burrows, M. T., Hobday, A. J., King, N. G., Moore, P. J., Sen Gupta, A., Moore, P. J., Thomsen, M.,  
 1004 Wernberg, T., and Smale, D. A.: Biological impacts of marine heatwaves, *Ann. Rev. Mar. Sci.*, 15 (1), 119-145,  
 1005 doi:10.1146/annurev-marine-032122-121437, 2023.
- 1006 Tassone, S. J., Besterman, A. F., Buelo, C. D., Walter, J. A., and Pace, M. L.: Co-occurrence of aquatic heatwaves  
 1007 with atmospheric heatwaves, low dissolved oxygen, and low pH events in estuarine ecosystems, *Estuar. Coasts*,  
 1008 45(3), 707-720, doi:10.1007/s12237-021-01009-x, 2022.
- 1009 Testor, P., de Young, B., Rudnick, D. L., Glenn, S., Hayes, D., Lee, C. M., Pattiaratchi, C., Hill, K., Heslop, E.,  
 1010 Turpin, V., Alenius, P., ... and Wilson, D.: OceanGliders: a component of the integrated GOOS, *Front. Mar. Sci.*,  
 1011 6, 422, doi:10.3389/fmars.2019.00422, 2019.
- 1012 Walsh, S. J.: Commercial fishing practices on offshore juvenile flatfish nursery grounds on the Grand Banks of  
 1013 Newfoundland, *Netherlands J. Sea Res.*, 27(3-4), 423-432, doi:10.1016/0077-7579(91)90043-Z, 1991.
- 1014 Wang, Y., Holbrook, N. J., and Kajtar, J. B.: Predictability of marine heatwaves off Western Australia using a linear  
 1015 inverse model, *J. Clim.*, 36(18), 6177-6193, doi:10.1175/JCLI-D-22-0692.1, 2023.
- 1016 Weller, E., Holliday, D., Feng, M., Beckley, L., and Thompson, P.: A continental shelf scale examination of the  
 1017 Leeuwin Current off Western Australia during the austral autumn–winter, *Cont. Shelf Res.*, 31(17), 1858-1868,  
 1018 doi:10.1016/j.csr.2011.08.008, 2011.
- 1019 Wolanski, E. and Kingsford, M. (Eds.): *Oceanographic processes of coral reefs: Physical and biological links in the*  
 1020 *Great Barrier Reef* (Second edition), CRC Press, Boca Raton, doi:10.1201/9781003320425, 2024.
- 1021 Woo, M. and Pattiaratchi, C.: Hydrography and water masses off the western Australian coast, *Deep Sea Research*  
 1022 *Part I: Oceanographic Research Papers*, 55(9), 1090-1104, doi:10.1016/j.dsr.2008.05.005, 2008.
- 1023 Woo, L. M. and Gourcuff, C.: Delayed Mode QA/QC Best Practice Manual Version 3.1 Integrated Marine  
 1024 Observing System, doi:10.26198/5c997b5fdc9bd, 2023.
- 1025 Wood, J. E., Schaeffer, A., Roughan, M., & Tate, P. M.: Seasonal variability in the continental shelf waters off  
 1026 southeastern Australia: Fact or fiction?. *Continental Shelf Research*, 112, 92-103, doi:10.1016/j.csr.2015.11.006,  
 1027 2016.